MASTER THESIS

Department Mineral Resources and
Petroleum Engineering, Chair of Petroleum
Production Engineering, Mining University of
Leoben.

By:
cand. ing. Georg Kain

Under the supervision of:
Prof. Dr. Dipl. -Ing. Wilhelm Brandstätter

Leoben, April 2009

Basic development of a fuel composition sensor

On behalf of

ICE Strömungsforschung GmbH
Hauptplatz 13
8700 Leoben

Leoben, April 2009

I declare in lieu of oath that I did this Master Thesis in hand by myself using only literature cited at the end of this volume.

_____

Georg Kain

Acknowledgements

First of all I want to express my deepest gratitude to my parents Waltraud and Alos Kain. They supported me in my whole lifetime and during my studies at the University of Leoben.

I would like to thank Prof. Dr. Dipl. -Ing. Wilhelm Brandstätter for supervising my thesis work and for supporting me in theoretical issues.

Special thanks to my tutor Dipl. Ing. Gernot Boiger for guiding me through this work and for his competent help.

Furthermore I want to thank Ing. Hermann Rainer for his advice and practical support in manufacturing the test set up.

Contents

List of figures

List of tables

Kurzfassung

Die gestellte Aufgabe umfasst die Entwicklung eines Treibstoffsensors auf optischer Basis, welcher die jeweils binären Mischungsverhältnisse von Diesel mit Biodiesel, Kerosin, Benzin, Cracked Gas Oil und Heizöl bestimmen kann. Die Entwicklung des Sensors unterlag einigen Rahmenbedingungen, da das Gerät Anwendung in der Autoindustrie finden soll. Die Diplomarbeit beginnt mit der Evaluierung verschiedener Optionen der Realisierung. Hierbei wurden im speziellen untersucht:

-Fluoreszenz Spektroskopie: Lumineszenz ist definiert als die Strahlung, welche ein Atom, oder Molekül abgibt, nachdem es Energie aufgenommen hat. Die wichtigsten Arten der Lumineszenz sind Fluoreszenz und Phosphoreszenz. Messung der Strahlung.

-Raman Spektroskopie: Es wird die Strahlung gemessen, welches ein Atom, oder Molekül aussendet, nachdem es Energie aufgenommen hat. Der Unterschied zur Lumineszenz besteht darin, dass die Elektronen in einen virtuellen Energiezustand versetzt werden. Messung der Strahlung.

-Dielektrizitätszahl Messungen: Jedes Material, welches zwischen den Platten eines Kondensators ist, besitzt eine Dielektrizitätszahl, welche die Kapazität bestimmt. Messung der Dielektrizitätszahl aufgrund der Änderung der Kapazität.

-Messung der Absorption von Licht der Probe: Jedes transparente Material besitzt spezifische Absorptionseigenschaften, die in einer Reduktion des transmittierten Lichtes resultieren. Messung des transmittierten Lichtes.

Nach dem Vergleich der genannten Optionen wurde entschieden, den Sensor auf Fluoreszenzbasis zu entwickeln, da hierbei die Erfolgsaussichten am größten waren. Für den Aufbau des Sensors war es daraufhin notwendig, einen Versuchsaufbau zu entwerfen. Dafür wurden die Komponenten und Eigenschaften des optischen Teiles bestimmt (Lichtquelle: LED, Photodetektor: Photodiode), sowie die Verstärkerschaltung entworfen. Diese Schaltung besteht aus einem Low-Pass Filter, zur Reduktion des AC Anteils, und einem nicht-invertierenden Verstärker. Nach ersten Testläufen stellte sich heraus, dass das

Fluoreszenzsignal zu schwach für die Detektierung war, weshalb die Methode fallen gelassen wurde. Da Messungen des transmittierten Lichtes auch mit dem schon vorhandenen Versuchsaufbau möglich waren, wurde auch diese Methode einer Versuchsreihe unterzogen. Die Absorptionsmessung in Kombination mit der Nutzung des Lichtbrechungseffektes an gerundeten Probebehältern, ermöglichte es die geforderten Mischungsverhältnisse mit einer Ungenauigkeit von <5% Abweichung zu bestimmen, weshalb die Aufgabenstellung als gelöst angesehen wird.

Abstract

The given task is about finding a proper way of detecting the mixing ratio of diesel with biodiesel, gasoline, fuel oil, cracked gas oil and kerosene. The development of the sensor was limited by given boundary conditions, because the device should be applicable in an automobile. This thesis starts with the evaluation of possible ways to realize the detector:

-Fluorescence spectroscopy: Luminescence is defined as the radiation, or light, emitted by an atom or molecule after it has absorbed energy. Radiation is detected.

-Raman spectroscopy: Generally Raman spectroscopy works in the same way as fluorescence spectroscopy. The main difference is that the electrons are not excited to an excited state, but to a virtual state. Radiation is detected.

-Permittivity measurement: Every substance located between the plates of a capacitor has a specific permittivity, which affects the capacity itself. The permittivity is measured by the change of the capacity.

-Absorption behavior: Every transparent material has a specific absorption behavior of light, which results in a reduced, transmitted light intensity. Transmitted light intensity is detected.

After the comparison of the named options, it was decided to realize the fluorescence spectroscopy option, because it had the biggest chance of success. The next step was the design of the test setup, with the selection of the optical components (light source: LED, photo detector: photodiode) and the design of the amplification circuit. This circuit is comprised of a low-pass filter, which reduces the AC component, and a non-inverting amplifier. After the first test runs, it became clear that the fluorescence signal was not detectable. Since measurements of the transmitted light were also possible with the existing test setup, several test runs were carried out. These measurements then provided good results. By the measurement of the transmitted light, it was possible to determine the fuel mixing ratios with a deviation of <5%. Because of the good results, the given task is assumed to be solved.

Introduction

The given task is about finding a proper way of detecting the mixing ratio of diesel and other fuels for an application in an automobile. There are some boundary conditions which limit the possible ways of realizing the detector:

- Low cost: The detector should not exceed 15€ in overall manufacturing cost.
- Small size: The detector must fit into the already narrow space of the engine compartment.
- Voltage consumption: The device must function under the standard car supply voltage.

The fuel detector is needed for the following tasks:

- The mixing ratio of Diesel and Biodiesel is important for an exact engine control.
- The detection of Diesel/Kerosene fractions impedes engine damage.
- Identification of erroneous refueling (e.g. Gasoline in a Diesel vehicle).
- Guarantee and warranty for engine damages can be given only, if correct fuelling was carried out, so the detector aids the ascertainment of claims.
- Getting information about Diesel and Fuel Oil fractions is interesting for tax authorities.
- Detection of adulterated fuel, especially in developing countries.
- Identification of the composition of fuel (Kerosene, Gasoline, Diesel,…) for multifuel engines; especially interesting for the military.
- Maintaining an exact mixing ratio of fuel and oil in two-stroke engines with oil-in-gasoline lubrication.

- The detection of synthetic fuels is important for the engine control.

Since it has not been clear, that the fluorescence detector is generally possible, alternative methods had to be dealt with, for getting an idea of different ways to solve the given task. Several methods have been looked into, evaluated and compared.

These methods are:

- Fluorescence Spectroscopy
- Raman Spectroscopy
- Permittivity measurements
- Absorption and Light scattering

Every method has its pros and cons, which are described in chapter 1. In addition to that, an overview is given about the applicability of the method for the fuel sensor. The absorption method is described in chapter 5.

At first, a fluorescence based detector was believed to be the most promising solution

The detector itself was developed based on the fluorescence method, which has a similar test setup to the absorption and light scattering method. The design of the test setup itself is described in chapter 3. After the first measurement runs, it turned out that the fluorescence signal was too weak for detection, so the absorption and scattering method was then applied.

The results are quite consistent in the outputs. Measurements were carried out with the following mixtures.

- Diesel/Biodiesel mixtures
- Diesel/Cracked gas oil mixtures
- Diesel/Gasoline mixtures
- Diesel/Kerosene mixtures
- Diesel/Fuel Oil mixtures

The latter liquids were mixed in 5%-10% concentration intervals. The voltage output for every measurement was recorded and analyzed for the standard deviation and average error. This analysis was carried out regarding the standard deviation of the measurement in relation to the average of all measurements on the one hand side, and the average error to the interval (lowest measurement voltage subtracted from highest measurement voltage) of all measurements on the other. For a detailed review of the results, see chapter 7.

According to the data acquired from the test runs, the task is believed to be solved, because of the low standard deviations of the measurements, and the comparable results of every test run.

It is stated here, that no correction factors are included in the analysis of the measurement results. For a review of possible error sources, see chapter 7.

A review of the results and recommendations are given in chapter 8.

1 Methods

Several potential, technical solutions have been studied, compared and weighed in terms of pros and cons. This chapter deals with different approaches for the given task.

1.1 Fluorescence Spectroscopy

Luminescence is defined as the radiation, or light, emitted by a molecule, or an atom after it has absorbed energy, which takes it to an excited state. The main types of luminescence consist of Fluorescence and Phosphorescence. [1]

1.1.1 General descriptions

One must distinguish between the electronic state and the electronic orbital.

An electronic orbital is defined as: "A partial description of the quantum state of an electron (or other particle) orbiting the nucleus of an atom. Different orbitals have different shapes and orientations, depending on the energy of the electron, its angular momentum, and its magnetic number. Orbitals have no clear boundaries; the shape of an orbital, as depicted graphically, shows only the regions around the nucleus in which an electron has a relatively high probability of being found. No more than two electrons (each with opposite spin) can coexist in a single orbital because of the Pauli exclusion principle." [2]

This means that the electronic state is a function, where an electron can be found with high probability. It is calculated by the wave function of a single electron, independent of other electrons.

An electronic orbital on the other hand is the combination wave function of all the electrons in all the orbitals of the molecule. [1]

Another important distinction is needed for the excited electronic state and the transition state. Transition states are in between the excited states, and correspond to energy in form of vibration. On the other hand side, the excited states have no further vibrational energy stored, but still have higher energy than the ground state and the underlying transition states. [1]

The electronic states can be divided into 2 groups, the singlet and the triplet state. The singlet state is characterized by the fact, that all the electrons have their spin paired. Triplet states have one set of electrons unpaired, which results in a lower energy than the singlet states, because of lower repulsion forces.

1.1.2 Quantum Energy

Light can only be absorbed in discrete packages, called Quanta, which is important for understanding the process of absorption. The energy carried by one quantum can be described as:

$$E = h\nu = \frac{hc}{\lambda} \qquad (1)$$

Where ν is the frequency, λ the corresponding wavelength and h = Planck´s constant (6,624 x 10^{-27} ergs/seconds).

The quantum is not constant as it is related to the frequency of the incident light. Table 1 shows the variation on the unit by different radiation sources.

Radiation	v (cm) (typical values)	Wave-number (μm^{-1})	Size of quantum (electron volts)	Size of einstein (kilogram calories)	Absorption or emission of radiation involves
Gamma rays	10^{-10}	10^{6}	1.2×10^{6}	2.9×10^{7}	Nuclear reactions
X-rays	10^{-8}	10^{4}	1.2×10^{4}	2.9×10^{5}	Transitions of inner atomic electrons
Ultraviolet Visible	10^{-5} 4×10^{-5} 8×10^{-5}	10^{1} 2.5 1.25	1.2×10^{1} 3.1 1.6	2.9×10^{2} 7.1×10^{1} 3.6×10^{1}	Transitions of outer atomic electrons
Infrared	10^{-3}	10^{-1}	1.2×10^{-1}	2.9	Molecular vibrations
Far infrared	10^{-3}	10^{-2}	1.2×10^{-2}	2.9×10^{-1}	Molecular rotations
Radar Long radio waves	10^{1} 10^{5}	10^{-5} 10^{-9}	1.2×10^{-5} 1.2×10^{-9}	2.9×10^{-4} 2.9×10^{-8}	Oscillation of mobile or free electrons

Table 1: Approximate sizes of Quanta [3]

This energy is very small and therefore a large amount of quanta are needed for excitation. Therefore it is more convenient to talk about the energy associated with N quanta. This number N is defined as the number of single molecules in a gram mole (Avogadro constant N = 6,624 x 10^{23}), and is called an Einstein (in photochemistry ONLY). One Einstein is the amount of energy carried by N quanta. So, if one molecule reacts by the absorption on 1 quantum (photon), then one Einstein is enough to make one mole gram react. A more practical example: in photosynthesis, the production of one mole oxygen needs 8 Einstein, if complete absorption of the incident light occurs (which is not possible) which means, 8 photons per molecule. The unit Einstein is not constant, since the amount of energy per Einstein is proportional to the size of one quantum, and thus to the frequency of the radiation (see table1).

The absorption of light produces excited molecules, which can then use the energy for dissipation, reaction or re-emission. Talking of luminescence, the quantum efficiency is defined as:

$$\phi E = \frac{number\ \ of\ einsteins\ \ emitted}{number\ \ of\ einsteins\ \ absorbed}\ or\ \frac{number\ \ of\ quanta\ \ emitted}{number\ \ of\ quanta\ \ absorbed}, \qquad (2)$$

which can never be larger as 1. [3]

1.1.3 Fluorescence Process

The basic principle of fluorescence is the excitation of electrons in a molecule to a higher energy state, by delivering energy in form of a specific wavelength radiation. The basic scheme is presented in Figure 1. Since the most stable state of an electron is the so called "ground state", which has the lowest energy, the excited electrons return to a lower energy state by relaxation.

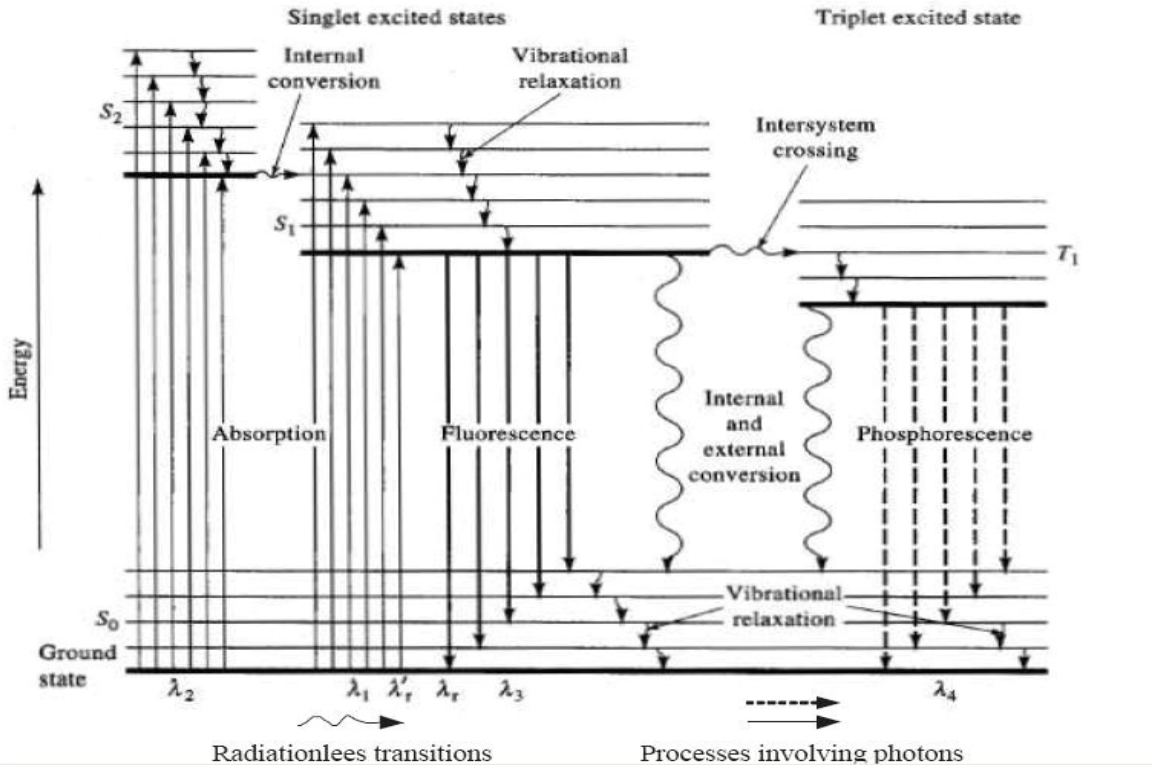

Figure 1: Basic principle of the fluorescence process [1]

Fluorescence only occurs as the electrons return from the last level of the excited state to an energy level of the ground state. The reason for that is the vibrational relaxation, which occurs virtually all the time. In this process, the excess vibrational energy is lost, as the electron returns to an excited state, because the energy is delivered in form of thermal energy to the environment. That is a very quick process, which only takes 10^{-13} to 10^{-11} seconds. So far no fluorescence occurs, since the energy differences are too small, and no energy is emitted.

The electron emits the photon as is jumps to a vibrational level of the ground state, where it relaxes further to the original ground state. The lifetime of an excited state, of the lowest state also, is approximately 10^{-9} to 10^{-7} seconds, which equals the fluorescence decay time.

The most important thing about fluorescence is the fact that the emitted photon has a lower energy than the absorbed photon, because of the relaxation process, so the emitted photon is shifted to a longer wavelength. This shift in wavelength enables the separation of excitation and emission light, and is called Stokes shift.

1.1.4 Internal Conversion

Since electrons can be excited to a higher excitation level than S_1, a process occurs, called internal conversion. In this process, the energy level of the lowest vibrational level of S_2 overlaps with a vibrational level of S_1, given that the separation of the energy levels is low. In this case, the electron will relax further without emitting any radiation. This is a very efficient path, which results in a very quick relaxation of the electron from S_2 to the lowest singlet state of S_1. Generally, one can say that the relaxation from any excited state to lowest singlet state in approximately the same time as the photon emission.

It could occur that electrons are relaxed by this process even further, down into the ground state, converting all the energy into heat. In this case fluorescence is completely disabled. The process of S_1 - S_0 conversion is not well understood, and almost impossible to measure, but it is assumed that only a very small faction of the molecules is relaxed in that way, wasting only little excitation energy.

1.1.5 Intersystem Crossing

Another observed phenomenon is the creation of triplet states out of singlet states. This mechanism involves a vibrational coupling between the lowest singlet state and the triplet state. The time needed for creating a triplet state is in the same magnitude as the lifetime of

the lowest singlet state, which makes the process possible. Intersystem crossing from higher energy levels than S_1 has not been observed, as the process can compete, speaking in terms of time, with fluorescence, but not with internal conversion, since the latter is too quick for allowing the creation of a triplet state. Generally, the lifetime of a triplet state is much longer than that of a singlet state (10^{-4} to 10 seconds).

Once the crossing has occurred, the electrons relax in the same way as in singlet state, with the difference, that triplet states generally have a lower energy, which can lead to complete relaxation to the ground state, again, disabling fluorescence. If an emission occurs, as the electrons jump to the ground state, it is called phosphorescence, which lasts as long as the lifetime of the triplet state. Because of the latter fact this phenomenon is also called the "afterglow" of the sample.

1.1.6 Synchronous Fluorescence Scan (SFS)

The creation of a SFS plot is quite similar to the EEM, but results in different contour diagrams. The SFS is created by scanning the emission of the sample at a fixed wavelength interval ($\Delta\lambda$) constant to the excitation. Expansion of the SFS with relative intensity results in a 3-D plot representing the total SFS (TSFS). Figure 7 shows a 2-D TSFS diagram of neat diesel.

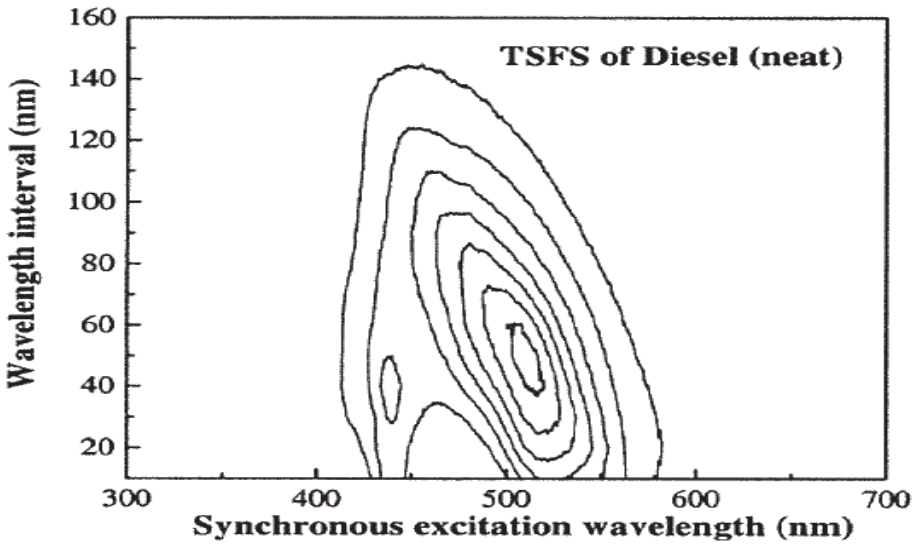

Figure 2: 2-D TSFS of neat Diesel [8]

As one can see, by comparing figure 2 and figure 6, the results are similar, since the relation between emission and excitation wavelength is:

$$\Delta\lambda em = \lambda ex + \Delta\lambda \quad (3)$$

The expanded 3-D TSFS plot can be seen in figure 3.

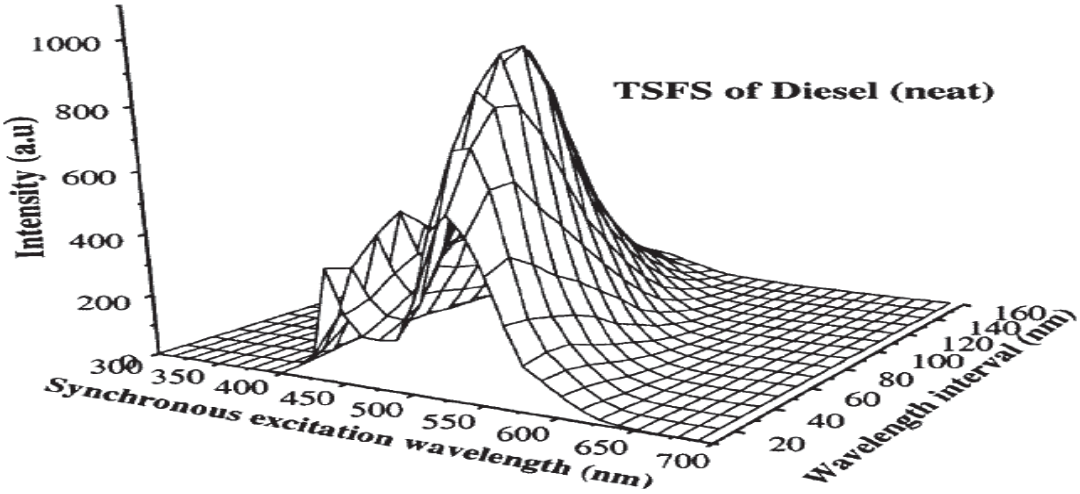

Figure 3: 3-D TSFS of neat Diesel [8]

The area beneath a spectrum represents the energy, emitted by the sample, so it was important to obtain intensity data for the EEM. Since there was no intensity data available, just for the TSFS, a graphical evaluation was necessary.

The following procedure was carried out:

1. Identification of the different intensity contours
2. Selection of a wavelength interval
3. Graphical elaboration of the intensities.

Figure 4 shows the procedure with colored lines.

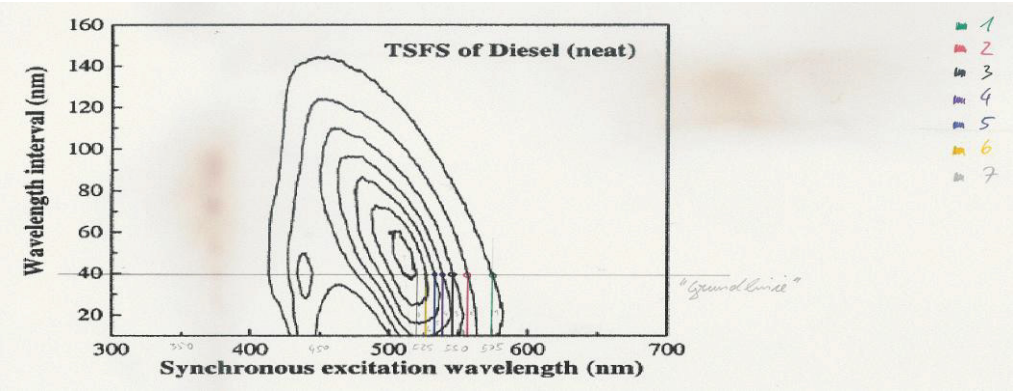

Figure 4: Wavelength evaluation [8]

From this plot, the corresponding wavelengths of the contour lines were taken. Since the contour lines of figure 2 and figure 6 are the same but are displayed in a different way, an excitation wavelength for a certain wavelength interval had to be found. The wavelength interval can be chosen freely because the intensity values are the same at every location for each contour line. The wavelength level of 40 was chosen, because there the relative intensity peak is reached, which then represents 100% intensity. The gained excitation wavelength information was then transferred to figure 3. The grid lines of the figure were then used, to gain the relative intensity data for the different contour lines.

Figure 5 shows the gained relative intensity information, where the heights of the colored lines at the wavelength interval of 40nm are then put into relation.

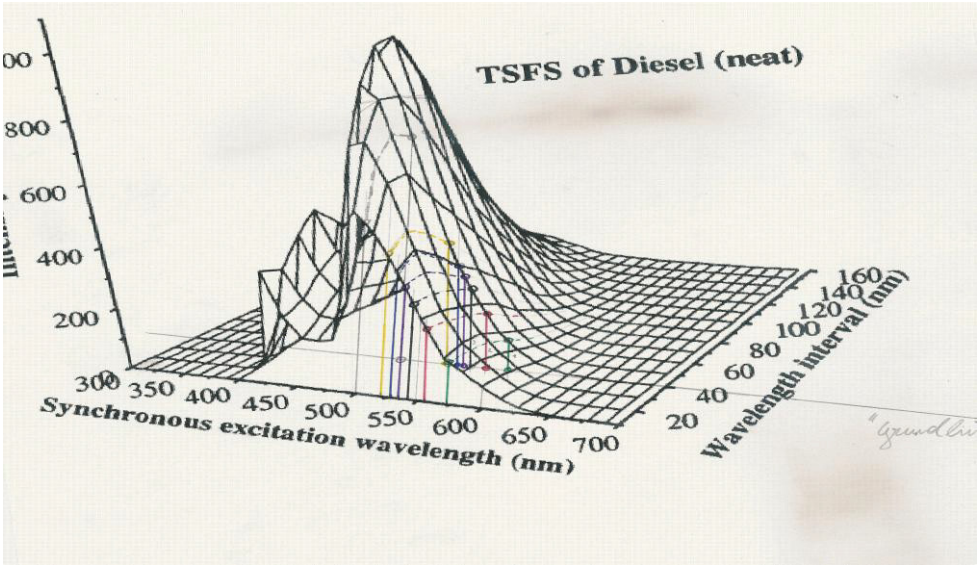

Figure 5: Intensity data evaluation for different contour lines [8]

After this procedure, it was possible to display a 3-D plot of the neat Diesel EEM

1.1.7 Practical application of fluorescence spectroscopy as a fuel detector

The creation of an Excitation Emission Matrix Fluorescence (EEMF) is a technique for obtaining a 3-D fingerprint of different samples. Patra & Mishra [6] carried out a full analysis of polycyclic aromatic hydrocarbons (PAHs) and petroleum products, for finding a relation between the measurements and the adulteration grade of the sample. Figure 6 shows an EEMF of neat Diesel, with measurement ranges of 5nm for each, excitation and emission.

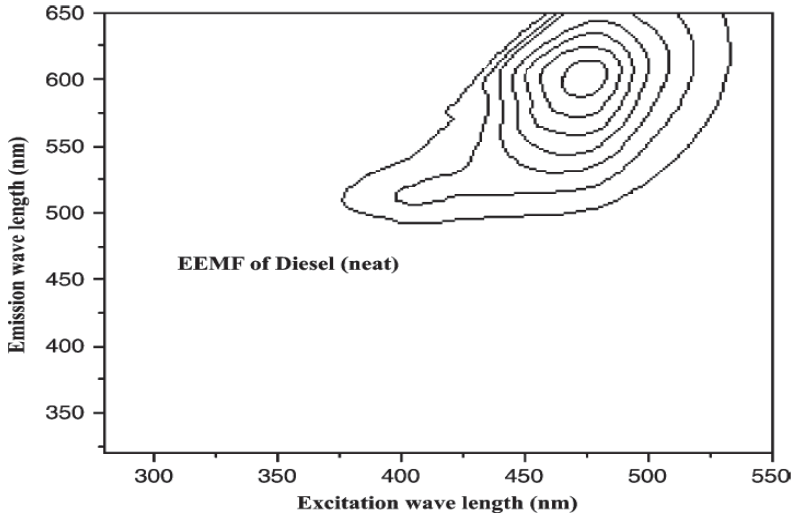

Figure 6: EEM of a neat Diesel sample [6]

These contour lines are obtained, by connecting the same intensity maxima at each excitation wavelength. From the above figure, one can see that an excitation wavelength of 475 nm seems to be the best option, since the emission intensity maximum is located around this interval.

Patra & Mishra [6] found out, that a simple EEMF of an adulterated sample is not sufficient for finding the type and grade of the pollution. Figure 7 shows a Diesel sample polluted with 5% v/v of Kerosene.

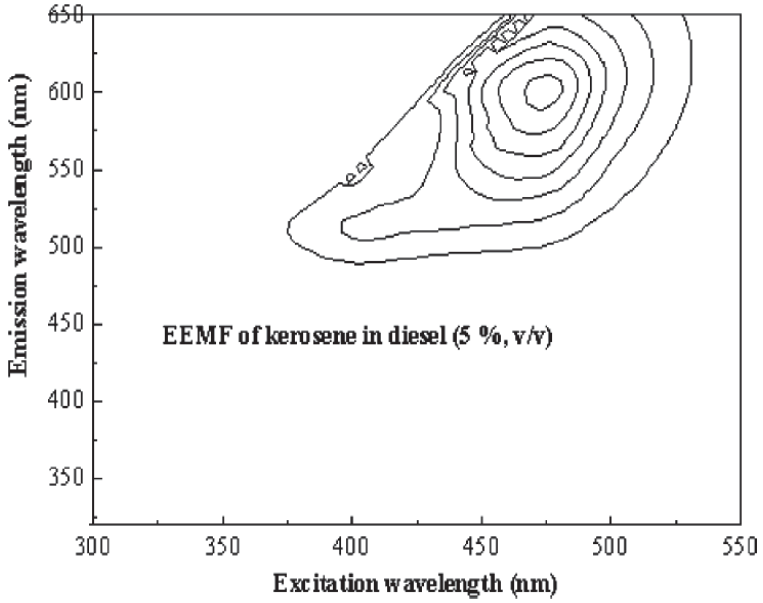

Figure 7: EEM of Diesel with 5% v/v of Kerosene [6]

As one can see by comparing figure 6 and figure 7, the difference of the shapes is not severe, just the intensities differ slightly from each other. Thus, it is useless for measuring the adulteration type and grade. Therefore an additional technique was necessary for enhancing the visible difference in the shapes of the samples. Patra & Mishra [6] then applied the Excitation Emission Spectral Subtraction (EEMSS). This means, that they subtracted the obtained EEMF of the polluted sample from the EEMF of the neat Diesel sample and created a new graph, shown in figure 8.

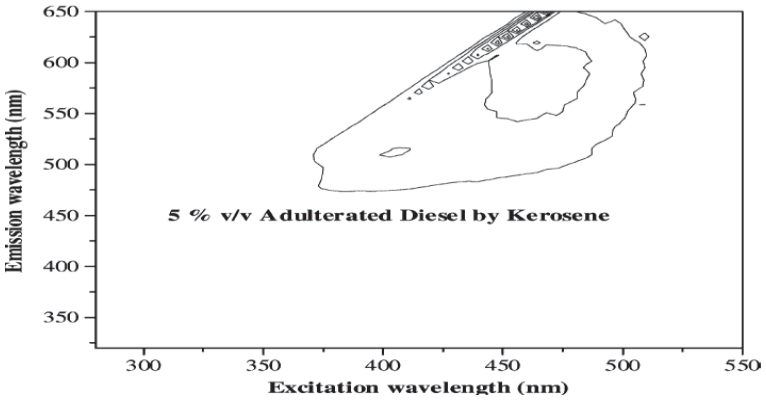

Figure 8: EEMSS of Diesel sample with 5% v/v of Kerosene [6]

Now the graph in figure 8 differs greatly from the graph in figure 6, which enables a qualified analysis of the adulteration grade and type. For obtaining suitable numerical values, which can then be compared, an integration of the 3-D EEMSS (EEMSS with intensity) of the polluted sample was carried out. This is just necessary for the polluted sample only, since the EEMSS of two neat samples does not give any result, only noise. The integration results in the EEMSS total volume, V_x, which has a relationship to the percentage of the adulterant as shown in figure 9.

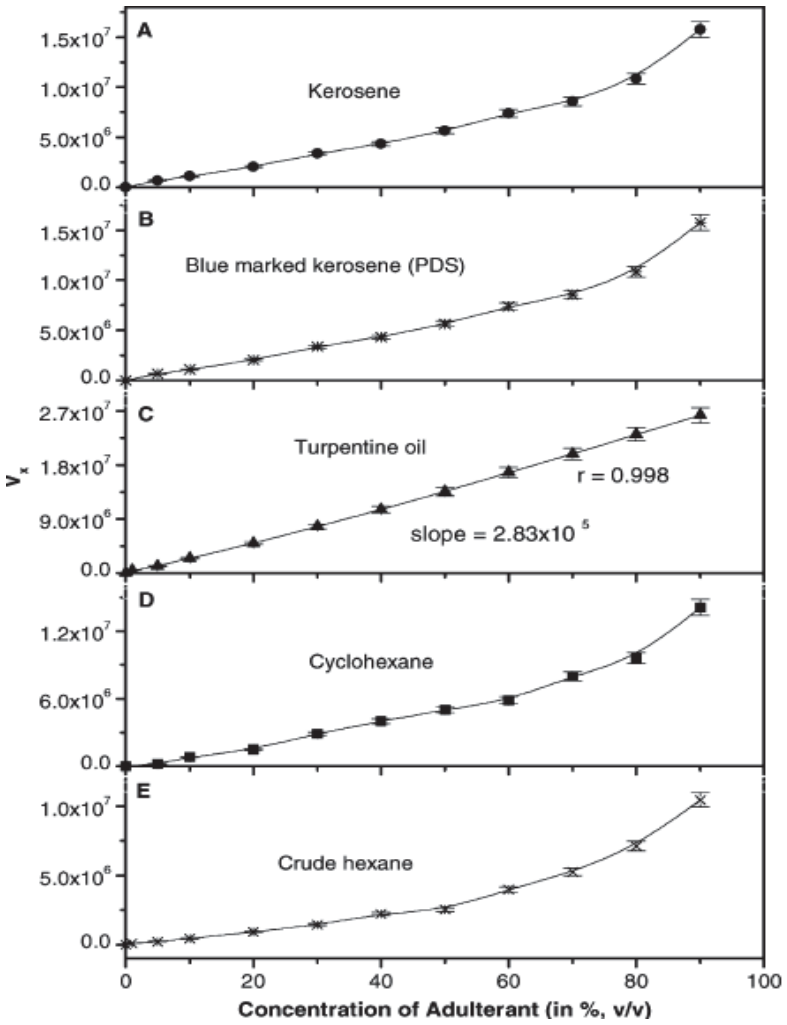

Figure 9: EEMSS total volume vs. adulterant concentration [6]

Now the grade of pollution can easily be obtained. The type of pollution cannot be determined, which means that this technique can be used for quantitative analysis only.

1.1.8 Field of Application

Since all organic compounds can be excited to fluorescence, it has a very broad field of application, which ranges from the food industry (quality control) to special logging tools in the oil industry (detection of oil and gas).

Generally spoken, the emission intensity of a polluted sample differs from the neat sample, which can then be correlated with the concentration of diesel/biodiesel. Figure 10 shows this effect on the example of the emission wavelength of a Diesel sample. The emission spectrum experiences a blue shift while it is polluted with kerosene.

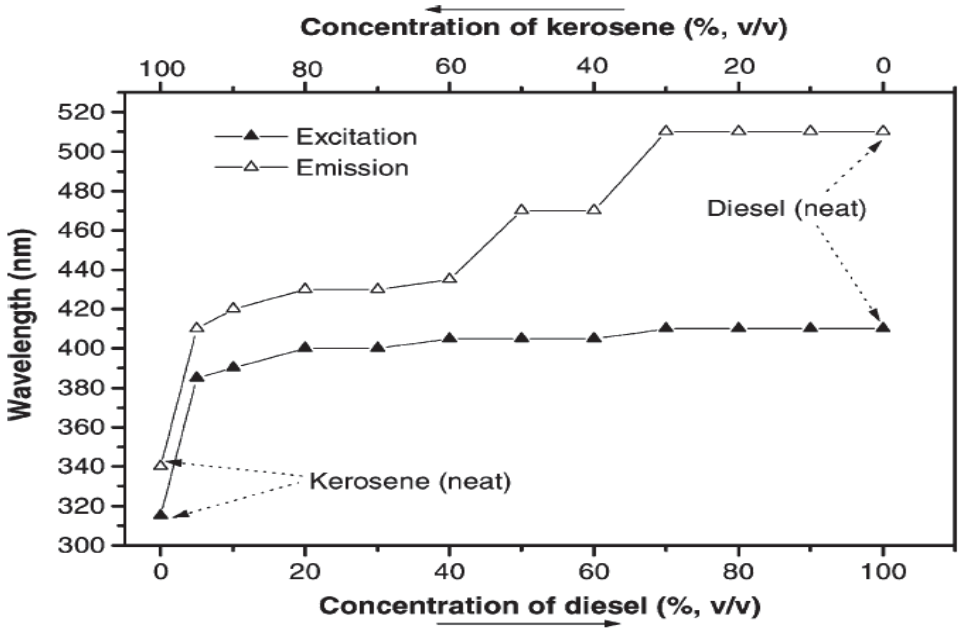

Figure 10: Blue shift of polluted sample [6]

1.2 Raman Spectroscopy

Generally Raman spectroscopy works in the same way as the fluorescence spectroscopy. The main difference is that the electrons are not excited to the first excited state, but to so called "virtual states" and return to ground state before reaching the excited states. This means that the emitted light is of even longer wavelength and lower intensity as it would be with fluorescence. The second reason for the lower intensity of the emitted light is the fact that most of the incident photons are elastically scattered (Rayleigh scattering) and only a small faction (1 in 10 million photons) is used for excitation.

Raman scattering was discovered in 1929 by V.C. Raman, who won the nobel price for his work. If a sample is excited by monochromatic light (Laser) the detected spectrum will consist of the following different lines:

- The excitation line is the strongest line, because it represents the original excitation light.
- The line with lower frequency than the excitation light is called the Stokes line.
- The line with higher frequency than the excitation light is called the Anti-Stokes line.

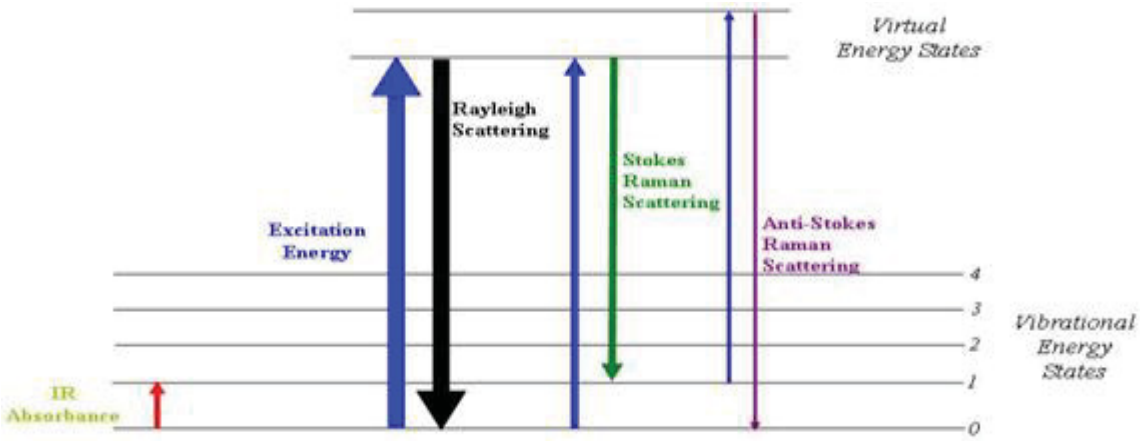

Figure 11: Raman excitation scheme [5]

As one can see from figure 11, the Rayleigh scattering returns the excitation light with no changes in the intensity and wavelength. The Stokes scattering returns the light at a lower wavelength, because the electron does not return to its original ground state, but remains in the first excited state.

The opposite case describes the Anti-Stokes scattering, where the electron is excited from the first excited state to the virtual energy level and returns to the ground state. This means that even more energy was emitted, than the originally used excitation energy. Despite this fact, the intensity of the Anti-Stokes lines is lower, because most of the electrons are originally located in the ground state, which do not create Anti-Stokes lines.

Normally, the Stokes shift is detected for analyzing the sample, but under certain circumstances, as for example poor detector response to low frequencies, the Anti-Stokes lines can be detected because of the higher frequencies and the similar information that can be gained.

1.2.1 Practical application of Raman spectroscopy as a fuel detector

Wayne Smith and Stuart Farquharson developed a fuel sensor based on Raman spectroscopy in the year 2006 (?) [7]. The initiator of this work was the U.S. military, which has had severe fuel supply problems during the invasion of Afghanistan and Iraq. Because of the quick advancement and huge fuel demand of the 24000 involved vehicles, the troops had to purchase fuel at regular gas stations. The problem then was that the foreign fuel was not compatible with the vehicles engines, which were damaged and stopped working properly. In order to avoid this problem in the future, Smith and Farquharson were assigned to find a proper and easy way for checking the fuel properties for its compatibility.

The Army´s already existing measuring technology were the Petroleum Test Kit (PTK), which was small, but limited in its measurement capabilities, and the Tactical Petroleum Laboratory, medium (TPLM). The latter was a laboratory trailer, with good analytical capabilities but a high demand in resources (hot water, power generator, ect.).

The task then was to develop a measurement kit, with the size of the PTK and the fuel measurement capabilities of the TPLM. Ultimate goal of the work was a quick, accurate test of an unknown sample, resulting in a simple statement about what the sample is (diesel, gasoline or jet fuel) and if it is suitable for use in vehicles.

Since petroleum fuels represent different crude oil factions distilled at various temperatures, containing aromatic, saturated, unsaturated branched and straight chained hydrocarbons, the Raman spectrum shows different peaks for the latter named properties. Figure 12 shows Raman spectra of the 3 primary fuel classes, diesel, gasoline and jet fuel.

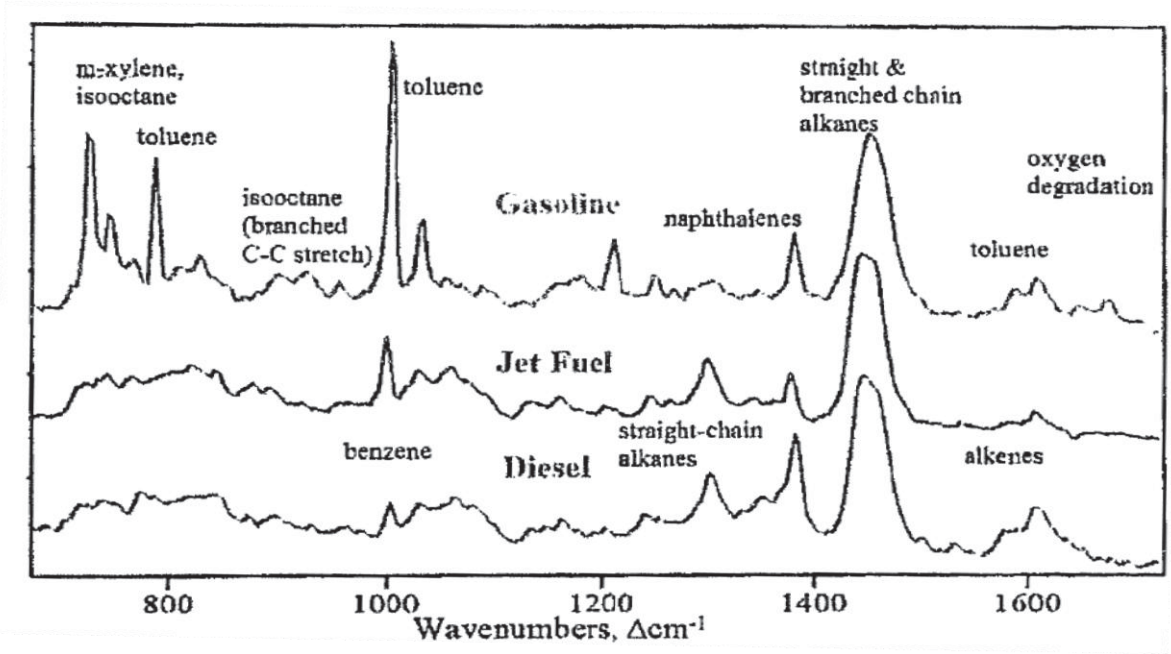

Figure 12: Raman spectra of diesel, gasoline and jet fuel [7]

By testing over 500 samples of diesel, gasoline and jet fuel from around the world, they identified 7 key product properties, which can be measured by Raman spectroscopy:

- Density
- Viscosity
- Cetane index:
  measurement of the combustion quality of diesel fuel during compression ignition
- Flash point:
  lowest temperature at which a flammable liquid can form an ignitable mixture in air
- Cloud point :
  temperature below which, wax in diesel or biowax in biodiesels form a cloudy appearance, and forms a solid phase
- Boiling point:
  temperature at which the vapor pressure of the liquid equals the environmental pressure surrounding the liquid
- Freeze point: the temperature range at which the sample changes state from liquid to solid

These 7 key properties determine the type and quality of the sample and its usability in U.S. vehicles. The developed Raman device successfully identified 31 unknown samples at different locations, so it is a suitable fuel detector.

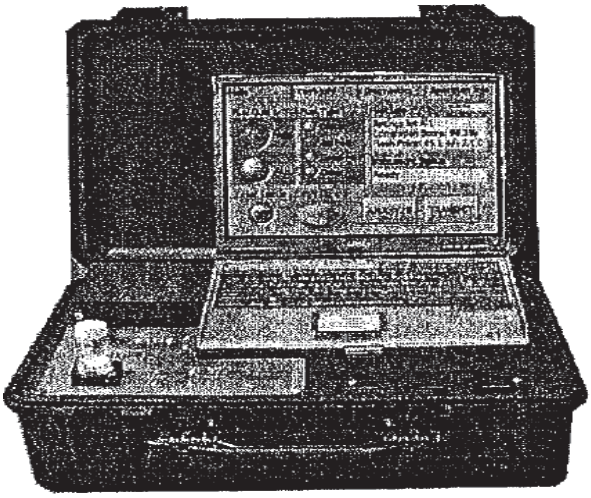

Figure 13: Portable Raman spectrometer [7]

1.2.2 Field of Application

Raman spectroscopy is used for identifying minerals and liquids. This method is very quick and effective, as molecular bonds can be identified additionally to the "normal" Raman spectra. General values for different bonds can be found in figure 14. From the results of laboratory measurements, one can create "fingerprints" for different compounds, which make a quick re-identification possible.

Frequency Range (in cm^{-1})	Band Assignment	Remarks
2700-3100	C-H alkyl free vibrations	Medium intensity in Raman
2230	C≡N stretch	very strong band in Raman, found in most cyanide based compounds
2190-2300	C≡C (triple bond stretch)	very strong in Raman
2100-2140	C≡C (triple bond stretch)	very strong in Raman
1650-1750	C=O stretch	Ketones appear on the lower wavelength side, aldehydes appear on the higher side
1600-1675	C=C stretch	Very strong in Raman
1580-1620	C=C stretch	Very strong in Raman
990-1010	Aromatic ring breathing	Appears at 992 cm^{-1} for benzene, around 1004 cm^{-1} for toluene.
650-850	C-Cl stretch	Strong in Raman

Figure 14: Raman values for different bond types [4]

1.3 Permittivity measurement

Permittivity is a physical quantity that describes how an electric field affects, and is affected by a dielectric medium. It is determined by the ability of a material to polarize in response to the field, and reduce the total electric field inside the material by that. Thus, permittivity relates to a material's ability to transmit (or "permit") an electric field. For example, in a capacitor, an increased permittivity allows the same charge to be stored with a smaller electric field (and thus a smaller voltage), leading to an increased capacitance.

Munack et al. [9] tested different sensors for their ability to work as a fuel detector.

- Agilent sensor
- Agilent measuring cell
- Oil-sensor
- Holland sensor

1.3.1 Agilent sensor

The main components of this sensor are the network analyzer and the Agilent sensor HP 85070 C, which is then in contact with the sample. Figure 15 shows the principle configuration of the test setup.

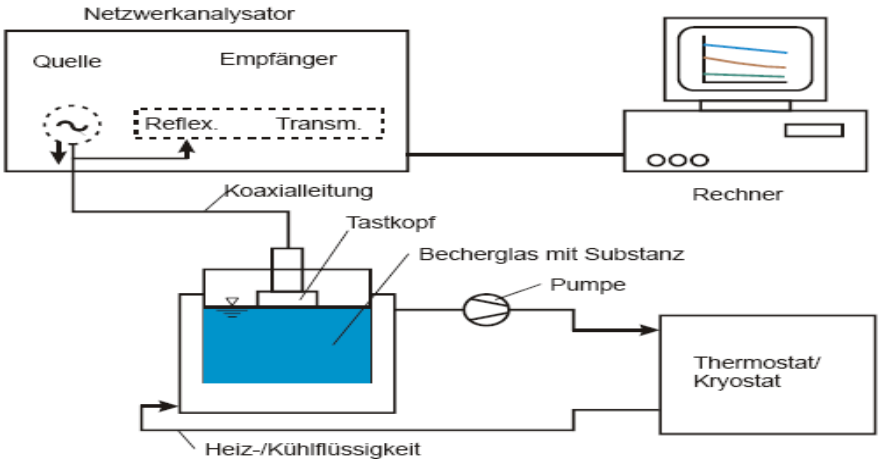

Figure 15: Principle Agilent test setup [9]

The main purpose of this setup is the measurement of permittivity values for different mixtures of Diesel and Biodiesel. The measurements have shown that the values were more or less constant with measurement frequency, but are temperature dependent. The Agilent sensor is for laboratory purposes only because of the hardware size. The results of the measurements at 5^0C are given in figure 16.

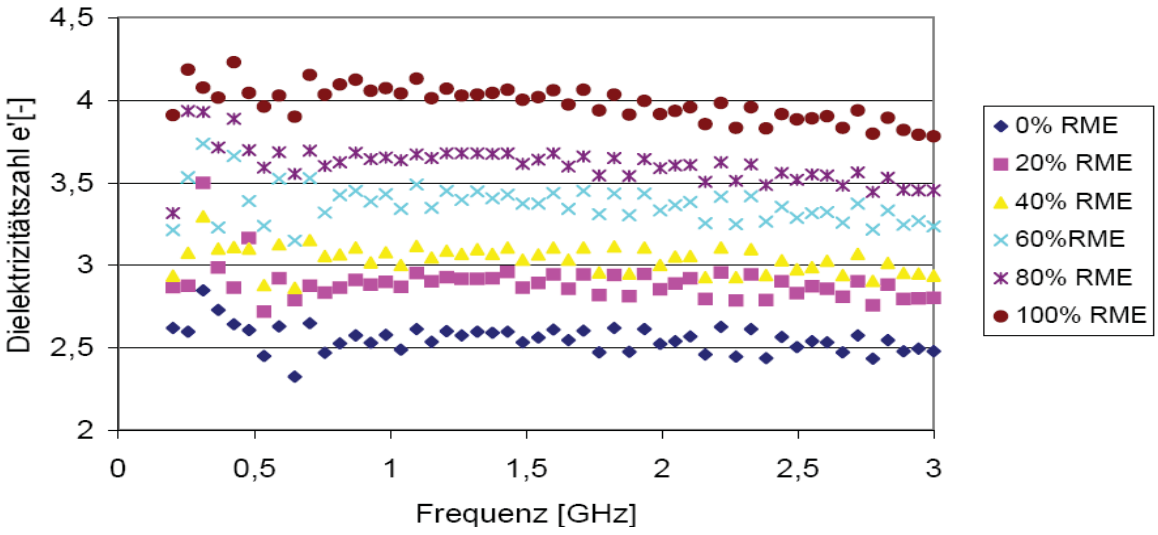

Figure 16: Agilent sensor (5 deg C) measurement results [9]

As one can see from the above figure, the test results are inaccurate at low test frequencies, which make the measurement useless. At a value of 0.8 GHz, the results become linear. The Agilent measuring cell was implemented, for getting accurate output values at low frequencies

1.3.2 Agilent measuring cell

The test setup for the Agilent measuring cell is similar to the original sensor. The main difference is the new scanning unit, the HP 16452A. Because the original test setup was not suitable for that new unit, an entirely new sample holder and new analysis software had to be developed. For a detailed review of the development process, see reference 9. After the preprocessing of the equipment, test runs were carried out with results shown in figure 17.

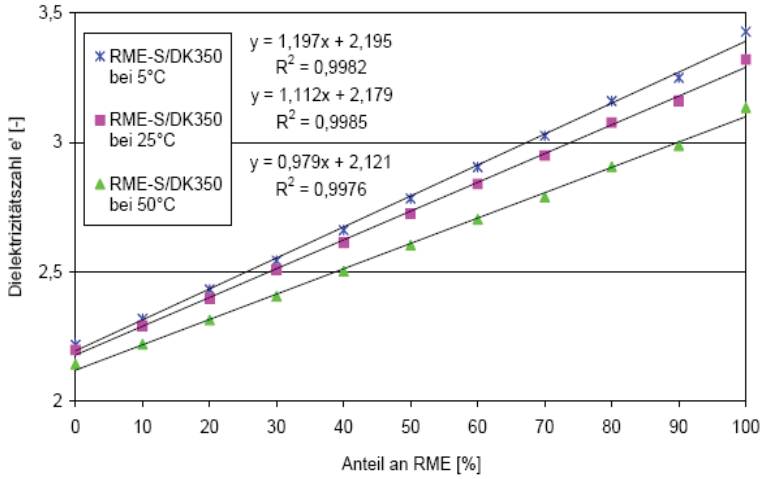

Figure 17: Measurement results, Agilent measuring cell [9]

The results show a linear behavior in relation to the composition, and are valid to be used for temperature correction.

1.3.3 Oil sensor

The 3rd evaluated permittivity sensor was the oil sensor, allocated by the Volkswagen AG. This sensor was originally designed for evaluating the chemical wear of motor oil in a combustion engine, but works with the same technique as the other evaluated methods. Figure 18 shows the outside look of the sensor.

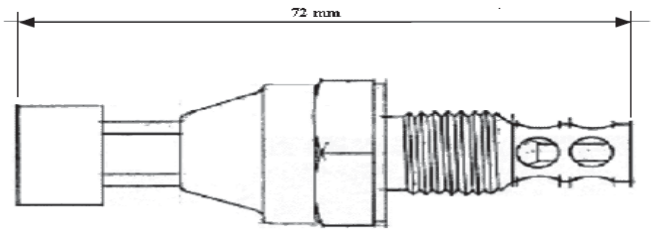

Figure 18: Oil sensor [9]

It is designed as a screw-in part, where the capacitor plates are on the inside, slightly above the slotted part of the above figure. These plates always have the same distance to each other, where the Diesel/Biodiesel mixture forms the dielectric medium in between.

The oil sensor works with a supply voltage of 5V, producing a sinusoidal output signal, with the exact analysis procedure not being released by Volkswagen. But it is stated, that the signal changes with the Diesel/Biodiesel fraction linearly, so it can be used for the given task. Figure 19 shows this behavior. One can also see the constant signal behavior at high Biodiesel factions.

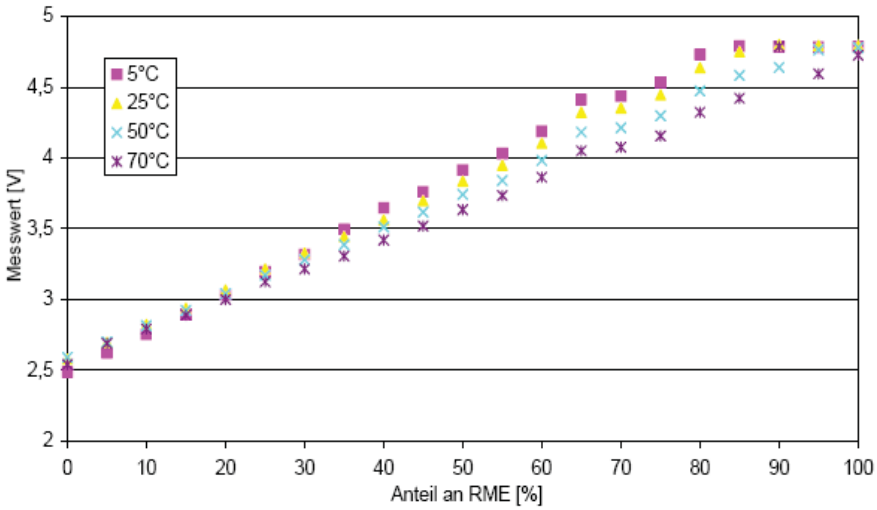

Figure 19: Oil sensor behavior [9]

The biggest problem is the fact that the output signal remains constant at low temperatures combined with a high Biodiesel percentage, since the maximum output voltage is then reached. Another problem was found, as the sensor was put on a long term measurement cycle. There the signal faded over time, making the measurement useless. It is stated, that this degradation of the signal does not arise from the sensor itself, but from the voltage supply adapter. The error results in a deviation of the measured Diesel/Biodiesel faction of 1%. Figure 20 shows the fading of the signal but take note of the high resolution of the y-axis, showing an error of 0,03V from the start to the end of the test cycle.

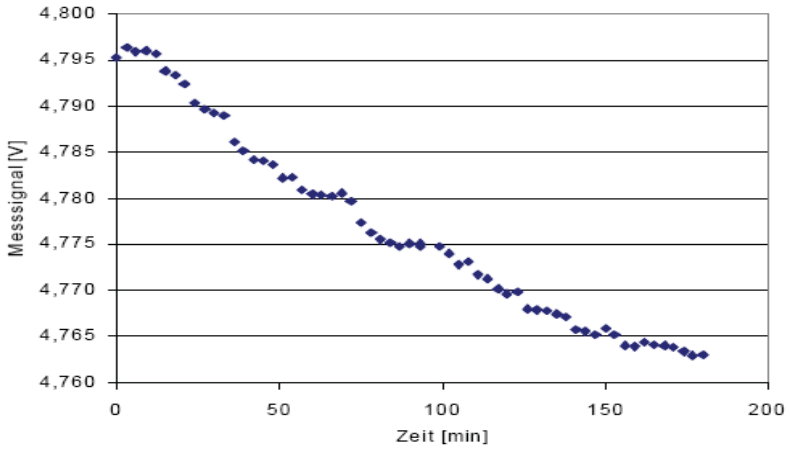

Figure 20: Oil sensor output signal fading [9]

Special account for the energy supply must be taken for an application as a fuel sensor in an automobile.

1.3.4 Holland sensor

This sensor was originally developed for measuring the relative permittivity of the ground. Figure 21 shows the Holland sensor. Generally this device measures the permittivity number of the test medium as well as the conductivity. The latter one is almost zero for a fuel medium, which makes the information useless.

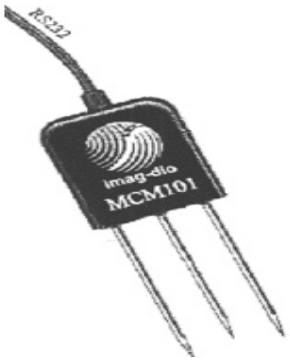

Figure 21: Holland Sensor [9]

With the gained information, one can calculate the humidity of the soil. The pins of the device are put into the ground, where the combination pin-soil creates a capacitor. Since the housing of the device was not RME resistant, a PVC disk is put onto the sensor, for separating the housing from the test liquid. Now the sensor is put into the test liquid, up to the half of the PVC disk. This results in a change of the measured signal, since now the signal is composed of the permittivity of the test liquid, air and the PVC. A complete analysis of the change was not carried out because the relative change of the permittivity was sufficient for the task. Figure 22 shows the result of the Holland sensor measurement for different temperatures.

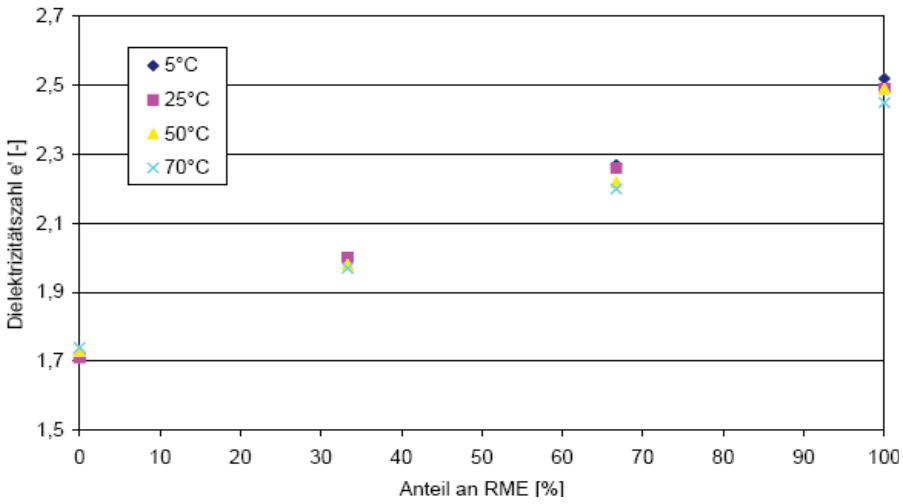

Figure 22: Holland sensor result for different temperatures [9]

As one can see, the measured values change insignificantly with temperature and show a linear behavior with increasing RME fraction.

1.3.5 Sensor Realization based on Permittivity

After the evaluation of the different possibilities, Munack et al. [9] decided to manufacture a sensor based on the discussed approaches but in 2 different variations:

- Flow-through design (figure 23)

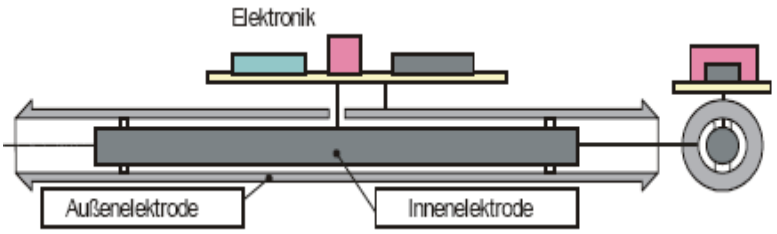

Figure 23: Flow-through sensor, side view, front view [9]

- Srew-in design (figure 24)

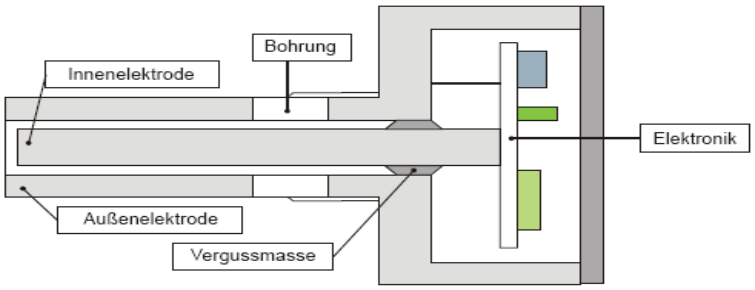

Figure 24: Screw-in sensor [9]

Both types work in the same way, with an inside, and an outside electrode, with the RME/Diesel mixture in between. The Flow-through sensor is placed on the fuel supply line, whereas the Screw-in sensor is located at the fuel filter. Both were applied in a car for a real life, long term test run. Both sensors detected the same RME concentration (temperature corrected) over time, until the Screw-in sensor failed, with no more sent data received. Table 2 shows the test results with analyzed and detected RME values. Note that the Screw-in sensor failed during the test, so Flow-through sensor data is shown only.

Probe Nr.	Datum	Uhrzeit	IR-Analyse [% RME]	Zeitpunkt Sen-sormessung	Sensor [% RME]	Sensortyp, Bemerkungen
1	04.10.2002	..	33.5	04.10.02 9:38	34.0	Einschraubsensor
2	06.10.2002	..	47	..	..	..
3	17.10.2002	..	26	17.10.02 11:55	26.9	Einschraubsensor
4A	29.11.2002	..	15	..	55.0	Aus Tank
4B	02.12.2002	..	55.0	04.12.02 5:57	55.0	Aus Kraftstoffleitung Einschraubsensor
5	18.12.2002	07:30	72.5	16.12.02 16.28	73.2	Durchflusssensor
6	20.12.2002	18:00	38.0	20.12.02 14.52	34.4	Durchflusssensor.
7	24.12.2002	10:00	77.0	24.12.02 12.02	76.1	Durchflusssensor
8	28.12.2002	11:00	88.5	26.12.02 12.58	85.6	Durchflusssensor
9	29.12.2002	16:00	54.5	29.12.02 14.59	54.3	Durchflusssensor
10	02.01.2003	..	37.0	04.01.03 12.42	36.3	Durchflusssensor
11	07.01.2003	17:00	80.5	07.01.03 16:36	79.0	Durchflusssensor
12	09.01.2003	20:00	34.0	09.01.03 14:42	33.3	Durchflusssensor
13	09.01.2003	..	18.0	10.01.03 14:52	17.6	Durchflusssensor
14	10.01.2003	..	7.0	10.01.03 7:46	8.6	Durchflusssensor
15	18.01.2003	..	52.0	21.01.03 8:02	52.8	Durchflusssensor
16	23.01.2003	..	86.0	22.01.03 6:33	85.1	Durchflusssensor
17	30.01.2003	..	21.0	29.01.03 16:53	21.8	Durchflusssensor
18	04.02.2003	12:00	72.0	04.02.03 14:50	74.1	Durchflusssensor
19	07.02.2003	12:00	32.0	07.02.03 7:25	34.8	Durchflusssensor
20	09.02.2003	11:10	22.0	08.02.03 13:23	24.9	Durchflusssensor
21	13.02.2003	..	6.0	13.02.03 18:48	11.9	Durchflusssensor
22	15.02.2003	10:05	70.0	15.02.03 8:41	70.6	Durchflusssensor
23	16.02.2003	15:10	81.0	17.02.03 15:36	82.3	Durchflusssensor
24	19.02.2003	..	20.0	20.02.03 6:11	23.0	Durchflusssensor
25	15.03.2003	..	40.0	14.03.03 17:52	44.8	Durchflusssensor
26	21.03.2003	..	53.0	20.03.03 13:50	56.5	Durchflusssensor

Table 2: Comparison of analytical and measured data [9]

As one can see, the analytically gained information (IR- analysis) corresponds to the measured data with sufficient accuracy, which made the project a success.

2 Review

The following section deals with a discussion about the advantages and disadvantages of the different methods.

2.1 Fluorescence Spectroscopy

If one now excites a fuel sample at a specific wavelength, and changes the composition of the sample, an emission light detector will detect a change of absorbed fluorescence emission energy. That's because the emission wavelength of the characteristic fluorescence intensity peaks of the sample vary according to the composition (red/blue shift).

The equipment of a sensor for the above task is relatively simple. It is generally composed of 3 sections:

- Excitation light source
- Emission light detector
- Electronic filter and Amplifier circuit

The voltage measurement is carried out by a commercially available Multimeter.

The first major advantage of a fuel detector based on fluorescence is the fact that it is not vibration sensitive. The second advantage is the small and available equipment, as stated above.

Major drawback of the method is the intensity of the emitted light, which is low and therefore hard to detect, which makes the selection of the emission light detector crucial, and possibly very expensive.

2.2 Raman Spectroscopy

Since Raman spectroscopy is widely used for mineral and fluid composition detection, it can also be used as a fuel detector.

The major advantages are the quick analysis procedure and the high accuracy of the measurement. Despite the high accuracy, Raman spectroscopy is not suitable for the given task, since it is highly vibration sensitive, which makes it unusable for application in an automobile. Moreover, the Raman device developed by Smith and Farquharson had the size of a suitcase (see figure 13), which was the smallest achievable size.

In addition to the vibration problem, the use of a laser in the engine compartment is not plain sailing, because of the laser´s energy demand.

The data analysis also poses a problem, since it would exceed the car computer´s capabilities.

2.3 Permittivity measurement

This measurement represents a very accurate and quick fuel detection method. As shown in section 2.3, it has already been developed and tested, which results in copyright problems.

The second drawback is the very high laboratory capability and time demand for developing an alternative for the already tested possibilities by Munack et al. [9]. The high temperature dependency of this method is also hard to come by, again because of the high complexity of the laboratory measurements.

2.4 Result

Based on the review of these three measurement methods, it was decided to attempt the construction of a simple, easy to use fluorescence device.

3 Test Setup Development

This section deals with the development of a test setup for checking the suitability of the fluorescence method as a fuel detector, split up into the different necessary steps.

Figure 25 shows the initial schematic test setup.

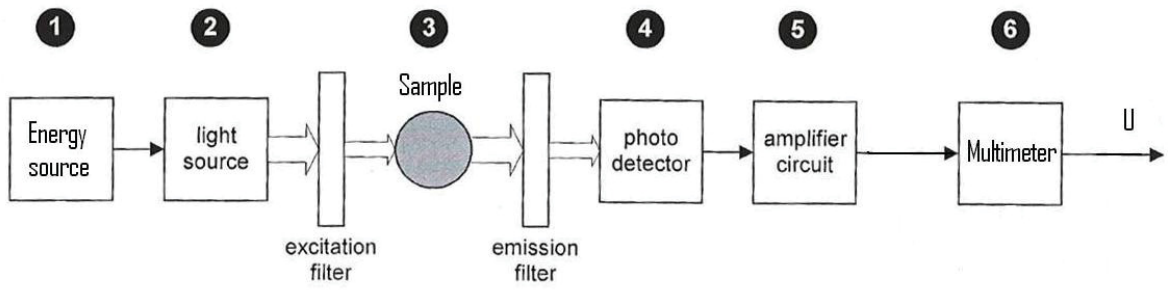

Figure 25: Schematic Test Setup (adapted from [13])

According to the above figure, every part of the device is described in the following chapters. The utilization of the excitation and emission filter can be avoided by selecting the light source and the photo detector according to optical characteristics which do not allow excitation light to be detected, which means that the photo detector´s spectral range must be outside the wavelength interval of the light source.

3.1 Energy Source

According to the specification given by the client, a 5V source is necessary. In the realized test setup, this was achieved by a simple network adapter, which reduces the common 220V line voltage to 5V.

3.2 Light Source

The light source is a major factor in the application, since the emitted light (wavelength) is directly responsible for the optical behavior of the sample. The best options for the described application are LEDs because of their little cost and optical characteristics, in other words, their narrow wavelength spectrum. For a first test of the device a LED with a main wavelength of approximately 470nm is believed to be a good choice because of the excitation-emission behavior of neat diesel as shown in figure 6.
Because of the latter criterion, the L-7104 PBC-Z LED by Kingbright was chosen.

Figure 26 shows the optical behavior of this LED.

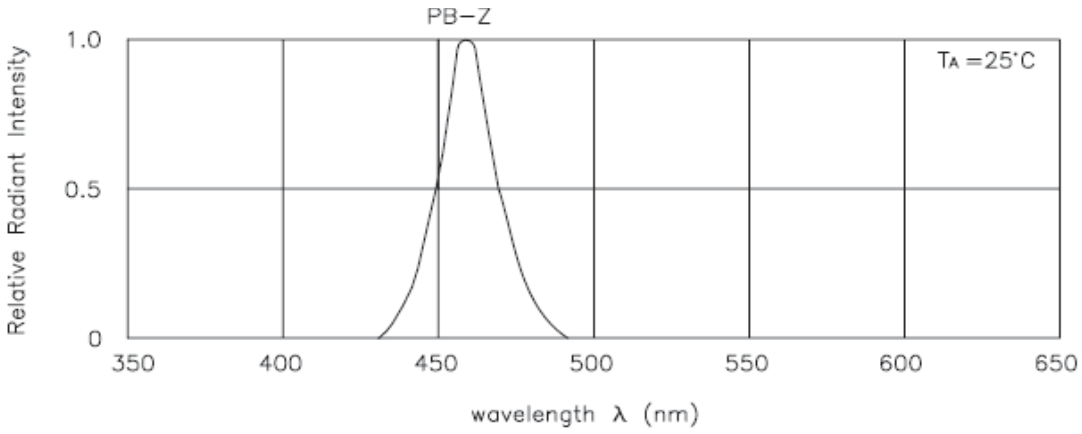

Figure 26: LED optical behavior [10]

As one can see, the relative intensity peak is located at the 465nm which is close to the expected optimum wavelength. Additionally, the energy demand of the LED is at 5V, which is also within the range demanded by the client. The L-7104 PBC-Z has a brightness of 2000 candela. This is an advantage, since the intensity of the light influences the optical behavior of the sample. The brightness can be controlled by a series resistor, applied between the energy source and the LED, which enables the possibility of carrying out test runs at a different brightness. Since LEDs are very sensitive to supply voltage changes, a series resistor should always be applied for minimizing the risk of LED damage because of energy supply fluctuations.

3.3 Optical Filters (excitation & emission)

In order to get a specific wavelength spectrum to excite the sample, a short pass filter should be applied between the light source and the sample. This filter "cuts off" longer wavelengths. Vice versa, a long pass filter positioned behind the sample then prevents short wavelength excitation light to reach the photo detector, which would make the test run useless.

In the case of Diesel, the excitation filter should be selected for extinguishing wavelengths above 480nm. On the other hand, the emission filter should repel any wavelengths below 490nm, for the reason stated above.

Generally, 3 different types of optical filters are available:

- Short pass filters (repel longer wavelengths)
- Long pass filters (repel shorter wavelengths)
- Band pass filters (only allow a specific wavelength interval to pass)

The major drawback of optical filters is the high costs. Because of that, the best solution for the given problem is to find an LED-photo detector combination which does not need

filtering for proper work. Such a combination can be selected freely, since the main requirement is, that the excitation light does not cross over with the bandwidth of the photo detector. A detailed data sheet can be found in the appendix.

3.4 Sample

The measurements were carried out with the test liquid inside 2 different sample containers:

- Square sample containers
- Round sample containers

This enables a comparison of the achieved results for the influence of the container form. Table 3 shows the basic sample container information

Square sample container:

- Manufacturer: Plastibrand
- Material: PMMA
- Dimensions: 12.5 x 12.5 x 45 [mm]
- Article number: 7591 15

Round sample container:

- Material: Glass
- Dimensions: Ø19 x 45 [mm]

3.5 Photo Detector

The best solution for a photo detector is a photodiode. These units convert the received light into a detectable voltage. Most important about the selection of the photodiode is the wavelength interval detected. As stated before, the interval must be selected in a way that the excitation wavelength is outside the detected interval. Since the LED has a wavelength of 465 nm, the photodiode must be selected with an interval above, or below. The better option in this respect is to select an interval above the LED spectrum, because a red shift is expected with RME. Since no photodiode with a perfect wavelength interval was available, the EPD-660-5/0.5 (by Epigap) and the EPD-520-5/0.5 (by Epigap) photodiodes were selected. The Interval of the EPD-660-5/0.5 is slightly too high, but should be sufficiently close to the desired interval for detecting at least a weak signal. The EPD-520-5/05 photodiode seems to be a good choice, because of the suitable wavelength interval.

Figure 27 shows the optical behavior of the EPD-520-5/0.5 photodiode.

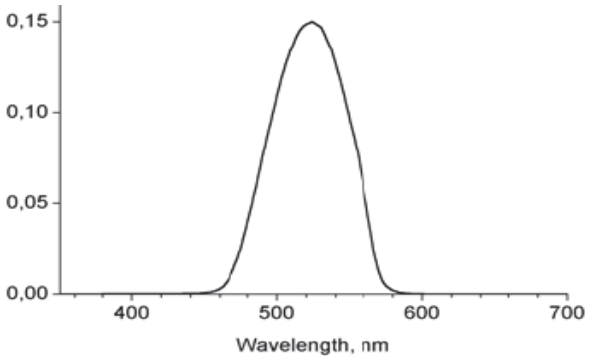

Figure 27: EPD-520-5/0.5 photodiode optical behavior [11]

The y-axis shows the responsivity in A/W. The data sheets can be found in the delivered CD.

3.6 Amplifier and Filter Circuit

The electronic part of the device is composed by 2 different parts, which are connected in series. These two parts are designed for

- Cutting off high frequencies, since the DC signal is of interest
- Amplifying the filtered signal.

3.6.1 Low Pass Filter

This electronic device is necessary, because the received signal is not DC voltage only. The AC part arises from fluorescence behavior, and fluctuations in the LED output. Since the test setup is intended for illuminating the sample continuously, small changes in the excitation light result in output signal alteration. These changes are also responsible for the so called "afterglow" (see section 1.1.5) of the sample, which superimposes the original signal.

Figure 28 shows a 1st order Low Pass filter, which has been realized in the test setup

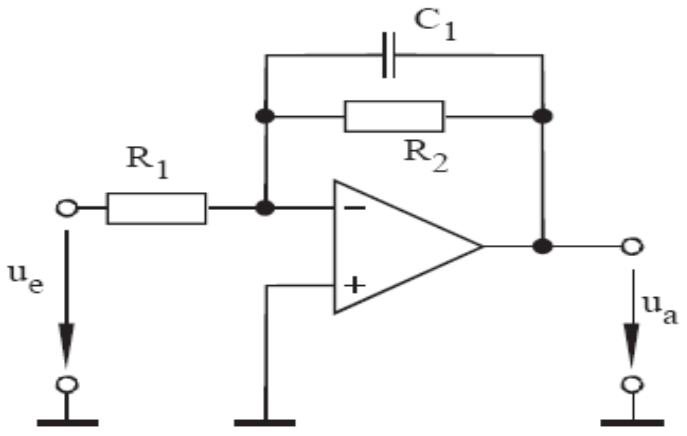

Figure 28: 1st order Low Pass Filter [12]

The transfer function equation of a 1st order Low Pass filter is:

$$A(P) = -\frac{{}^{R_2}/_{R_1}}{1+\omega_g \cdot R_2 \cdot C_1 \cdot P} \tag{4}$$

Where:

- R_2…..parallel resistor [Ω]
- R_1…..series resistor [Ω]
- ω_g…. frequency [kHz]
- C_1…..capacitor [nF]
- P…….standardized complex frequency variable [ ]

The resistors can be calculated as follows:

$$R_2 = \frac{a_1}{2\pi \cdot f_g \cdot C_1} \tag{5}$$

and

$$R_1 = \frac{R_2}{A_0} \tag{6}$$

In this case, the boundary frequency f_g [kHz] can be selected freely and should be as low as possible for eliminating most of the AC fraction, so the value 0,01kHz was selected. The capacitor C_1 [nF] can also be selected freely, according to the availability of the part, so a value of 10nF was selected. The amplification coefficient A_0 is 1 in this case, since the filter circuit is dimensioned independently of the upcoming amplification. The factor a_1 is a simple relation factor and can be selected freely again, here 1. Because of the named values and the used equations, it is obvious that R_1 and R_2 have the same value.

Inserting the values into equations 5 and 6, the result is:

$R_{1,2} = 1{,}59\ k\Omega$

3.6.2 Amplifier circuit

After the signal treatment by the Low Pass filter, an amplifier circuit enhances the voltage to a detectable level. The amplifier circuit design is complicated with many factors influencing the result.

Christian Kolle [13] carried out an extensive evaluation of the amplifier problem in his PhD thesis. The topic of this thesis was the development of a fluorescence device, which is able to detect oxygen in evacuated food packages. Since the fluorescence signal is always very weak, a large part of the thesis is used on amplification issues.

Kolle´s device works in a frequency modulated way, where the luminescence light is put into relation to a reference diode. The term "Frequency modulated" already indicated the usage of AC for the device. He found very nice amplification alternatives, which he evaluated extensively, always with focus on his main goal of finding an AC, low noise amplifier. Kolle designed the amplifiers as a High Pass filter in combination with an amplifier, because his goal was the detection of the AC signal only.

This made the application of one of his sophisticated amplifier alternatives for the fuel detector impossible, because it was not possible to convert them to DC mode. For a detailed review of Kolle´s efforts, please see reference 13.

After the time consuming and fruitless efforts to convert an AC amplifier to DC mode, it was decided to manufacture an alternative for testing purposes. The result was the application of a non-inverting amplifier. Figure 29 shows the amplifier configuration.

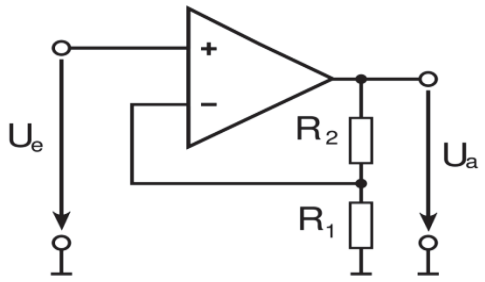

Figure 29: Non-inverting amplifier [14]

This amplifier enables a flexible change of the amplification factor A_0, because it is controlled by the resistors only and is calculated by equation 7.

$$A_0 = 1 + \frac{R_2}{R_1} \tag{7}$$

The output voltage is then

$$U_a = U_e \cdot \left(1 + \frac{R_2}{R_1}\right) \tag{8}$$

Since the AC part of the signal has proven to be negligible, no AC filtering unit was implemented in the actual test setup.

3.6.3 Combination Circuit

After the preparation of the 2 main parts, the combination of the filter and the amplifier was the next step. The plot was created with the PSpice software, which is available as a student version on the internet. This software is intended to simulate electrical circuits with parameters given by the user. Figure 30 shows the combination circuit as a PSpice plot.

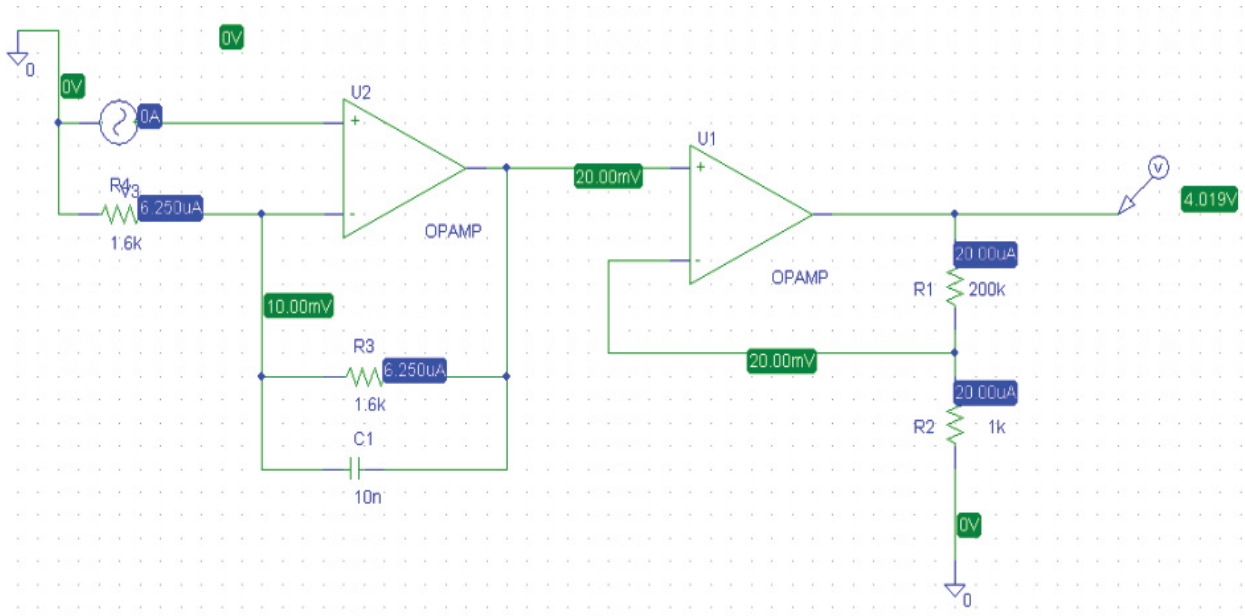

Figure 30: Combination Circuit

Since photodiodes are not included in the software, an AC/DC power supply was simulated, with an overall output of 10 mV. In the above figure, one can see the values the circuit was simulated with. Where e.g. 10n means 10 nF, or 1k means 1kΩ.

The applied OPAs are both OPA 604 (by Burr Brown). The OPA 604 model was selected, because of its good noise behavior and overall performance. The data sheet can be found in the appendix. The capacitor and the resistors are standard commercially available parts.

The manufacturing of the test setup was carried out in cooperation with Fischer E-Tech, Bad Goisern, Austria.

4 Fluorescence Results

After the manufacturing of the test setup, the first measurement runs were carried out.

It must be stated here, that the fluorescence signal was not detectable with the EPD-660-5/0.5, most probably because of the high wavelength interval of the photodiode. With the EPD-520-5/0.5 photodiode, which should be suitable for the application, too much excitation light was detected, making the measurement results useless, because the emitted light from the sample was then completely superimposed by the detected excitation light. In addition to that, it is assumed that the luminescence light was too weak for detection with the available equipment. Adaption of the test setup would result in a cost increase, which would make the application too expensive for mass production, because the only thinkable alternative for the photodiode, the Jen Colour MCS3AS, is too expensive for use, with an unknown behavior for the given task.

5 A new approach

After the 1st device failed to detect the luminescence light, because of the reasons stated before, an alternative way for the fuel detector had to be found. The first intention was the utilization of the extinction behavior of the samples since it was possible to re-use the already manufactured test setup.

5.1 Beer-Lambert law

The Beer-Lambert law describes the extinction behavior according to the equation:

$$E_\lambda = -\lg\left(\frac{I_1}{I_0}\right) = \alpha_\lambda \cdot c \cdot d \qquad (9)$$

where:

- I_1…..Intensity of the transmitted light [cd]
- I_0…..Intensity of the incident light [cd]
- c…..Concentration of the absorbing component in the liquid [mol/l]
- α_λ…Common extinction coefficient at a specific wavelength λ; is influenced by the ph value of the sample
- d…...Thickness (diameter) of the sample

The reduction of the incident light can also be described by equation 10

$$I_1 = I_0 e^{-\alpha^* \cdot c \cdot d} \qquad (10)$$

Rearrangement of equation 10 results in the relation for calculating the extinction coefficient, because the incident and the transmitted light can be measured and c and d values are known.

$$-ln\left(\frac{I_1}{I_0}\right) = \alpha^* \cdot c \cdot d \tag{11}$$

The transmitted light intensity can now be predicted with equation 10. The main problem now is found in the extinction coefficient, because values for the test liquids cannot be found. Recalculation of the coefficient with equation 10 only results in the value for the mixture, but not for the single components.

For receiving the extinction coefficient, equation 11 must be rearranged. The relation between the transmitted and incident light is not defined by the natural logarithm, but by the common logarithm. A linear relation between these two exists, as described in equation 12.

$$\alpha = lg(e)\alpha^* \approx 0{,}434\alpha^* \tag{12}$$

Inserting equation 12 into equation 11 results in

$$-lg\left(\frac{I_1}{I_0}\right) = \alpha \cdot c \cdot d \tag{13}$$

This enables a new way of realizing the fuel detector. The components of the binary mixture feature two different extinction coefficients α_A and α_B. The coefficient of the mixture α_M however relates to α_A, α_B and c via a previously unknown function, such as:

$$\alpha_M = f_M(\alpha_A, \alpha_B, c) \tag{14}$$

For any binary mixture, f_M can be determined by calibration experiments, as carried out in chapter 7.

5.2 Snell´s law

This law describes the behavior of light and other waves, as they pass through a boundary of two isotropic media. The law states that the ratio of the sines of the angles of incidence and of refraction light is a constant that depends on the media. This relation is described in equation 15.

$$\frac{\sin \varphi_1}{\sin \varphi_2} = \frac{v_1}{v_2} = \frac{n_2}{n_1} \tag{15}$$

or

$$n_1 \cdot \sin \varphi_1 = n_2 \cdot \sin \varphi_2 \tag{16}$$

where:

- φ…..angle of incident and refracted light
- v…..velocity of the light in the different media
- n…..refractive index, depends on the medium

If now a light ray crosses the boundary between e.g. air and water, the light wave will be slowed down in the denser medium, here the water. The angle at which the wave is refracted is measured from a normal line, which is perpendicular to the two media´s surfaces.

Figure 31 shows this behavior.

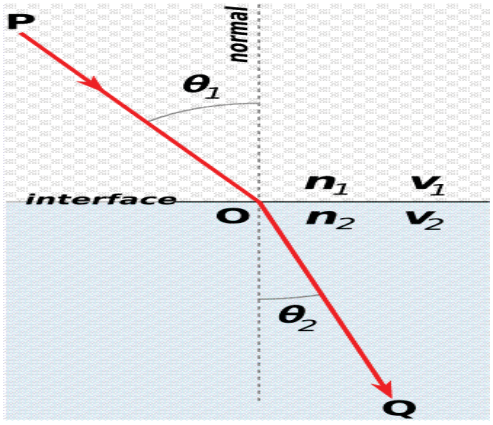

Figure 31: Refraction of a light ray [15]

The described behavior influences the results of the measurement, because the light ray is refracted.

5.3 Focusing of light

Focusing of a light ray, as it is sent trough a bent surface is also an important issue for the results of the measurement runs, as round sample containers were used.

Generally, the incident light is focused by a converging lens. Now, parallel light beams converge to a certain spot at a certain distance behind the lens, which is called the focal length. Round cylinders show the same behavior.

If the focal length of the round sample container is about the distance between the photo detector behind the container and the container itself, the output signal is enhanced.

This behavior is used in the test runs, as the unamplified signal is higher, reducing the need of the amplification itself.

The refraction behavior of the different samples aids the measurement. Every liquid has a special refraction coefficient, which determines the focal length of the sample itself.

Figure 32 shows this behavior in a simplified way.

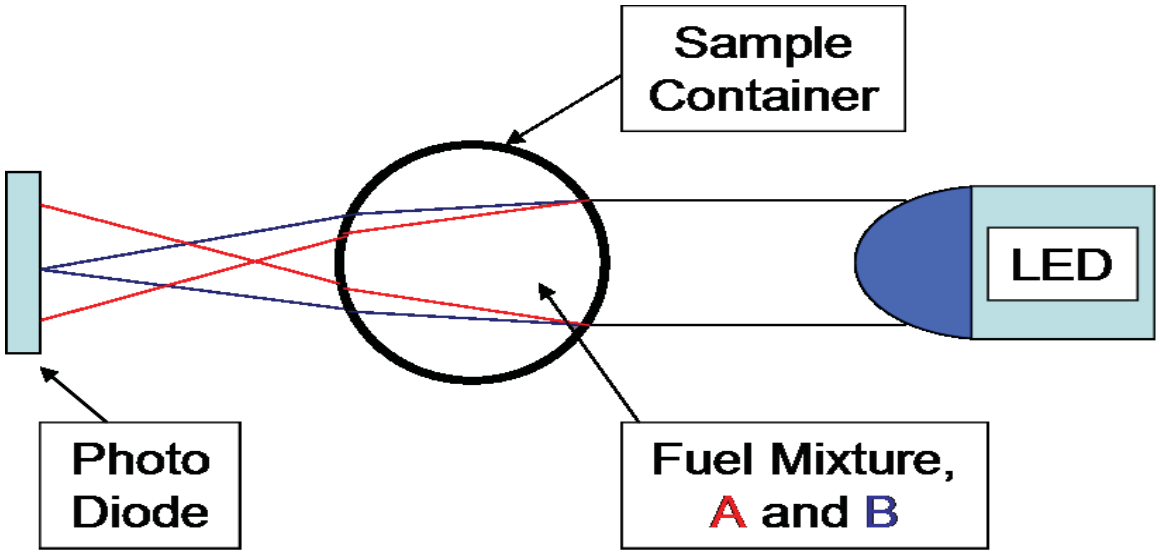

Figure 32: Refraction behavior of different samples

As one can see, the different mixtures create the focal point at a different length behind the sample. This causes a second, improving differentiating factor, as a change of the detected light in relation to the measured fuel mixture occurs. The absorption causes a voltage change in the output and the refraction behavior of the sample causes an additional change, since the focal point is positioned differently for every mixture fraction.

6 Measurement procedure

In this section, the measurement procedure is presented. The used measurement method of the fuel detector is the absorption and scattering behavior of the different samples.

In order to make the measurement runs reproducible, the measurement of a single sample is described, and must be repeated for all samples. The following steps have to be carried out for each and every sample:

- Sample preparation:
    - Cleansing of the sample containers:

      The containers should be cleaned by the use of water and soap for removing residues of earlier test runs. Check the sample containers for streaks. If there are no streaks visible, proceed. If streaks are found, repeat the cleaning procedure until no more streaks are visible.

    - Preparing the samples:

      Take special care for an accurate mixing ratio of the sample. The mixing for the measurements was carried out by the use of commercially available hypodermic syringes, which was not the optimal equipment. Small inaccuracies in the mixing ratio result in a large adulteration of the measured signal and can make an entire test run useless.

    - Sample control:

      Number the sample containers, so no samples can be skipped, or measured twice. Also revise the liquid levels of the samples, for identifying erroneously mixed samples, as all sample containers must have the same level.

Stratification of the samples can be observed because of different densities of the fuels. Mix the sample by shaking it after the named steps.

- Test Run
    - Setup preparation:

      Look for dust or other contaminations at the photo detector. Revise the sample holder for correct positioning of the sample.

    - Measurement:

      Activate the light source and put the sample into the sample holder. Close the hatch for creating a dark environment. This is very important, as any light from outside adulterates the result. Wait for the signal to stabilize (~10 sec)

    - Data acquisition:

      Record the voltage shown at the multimeter and put the value into a calculation program (e.g. Microsoft Excel ©), for further analysis.

Repeat the named procedure for every sample. The procedure can be accelerated of course e.g. by preparing the entire sample series at one time, etc.

As stated before, the sample was positioned 2cm from the light source and 2cm from the photo detector (metered from the outside of the sample container).

7 Results

This section deals with the acquired data from the measurement runs and the interpretation of the same. The measurements were carried out with both available sample containers (see section 4.4). The results are presented for the unamplified signal only, because the unamplified output voltage was high enough for accurate measurements. In addition to that, the possibility of detecting the unamplified signal increases the cost efficiency of the potential measurement device, so the amplification was left out. For analyzing the accuracy of the different measurements, the standard deviation was calculated with equation 17.

$$\sigma = \sqrt{\frac{1}{N-1}\sum_{i=1}^{N}(x_i - \bar{x})^2} \tag{17}$$

where:

- N….number of trials
- x_i….value of the i[th] trial
- $\bar{x}$.....average value

Here, the $\bar{x}$ is the overall average value of **all** test runs of an experiment

The analysis of the different fuel mixtures results was carried out in two ways:

- Average error based on the overall average:

  This average error is acquired by dividing the calculated standard deviation through the measured voltage values. It shows the deviation of the measured signals in relation to the average values of the measured voltages. This error will be quoted as the “value error”. The value is expressed in %.

- Average error based on the measured interval:

  Here, the average error is calculated based on the overall average standard deviation. The acquired sigma is then divided by the measured interval, which is the highest measured value minus the lowest measured value. The acquired value shows the deviation of the measured data in relation to the measured interval. This error will be quoted as the "interval error". The number is dimensionless, or expressed in %.

Very important for interpreting the quality of the results are the following points:

- No temperature correction was carried out

  The measurement of liquid properties is almost always highly temperature dependent, because of the density change. The results are presented with no respect to the temperature dependency.

- It was not possible to completely eliminate ambient light

  This means that the results can be influenced from outside light up to a certain degree.

- Chemical reactions are not accounted for

  The change of the absorption behavior of the test fuels, as they react with each other, is not included.

- Sample preparation errors

  Due to the fact that the samples were prepared by hand with commercially available hypodermic syringes, the mixing error could be an influencing factor. This is especially important for the square sample containers because of their low volume, where a droplet too much, or too few can already change the result. Nevertheless the preparation was carried out as accurately and carefully as possible.

- Bad cleaning of the sample containers

  The cleaning of the containers was carried out very carefully, but a complete elimination of this factor could not be guaranteed.

Always bear the named unaccounted factors in mind while reading the results. It is anticipated here that the round sample containers always gave better results in terms of reproducibility, than the square sample containers. Three main reasons are supposed to be the cause of that:

- Easier cleaning of the already used sample containers.
- Due to the higher volume of the round sample containers, the sample preparation can be carried out more accurately.
- Measurement effect due to the absorption behavior seems to be enhanced by the effect of refraction, which depends on the "lens effect" of the round sample containers and the refraction coefficient of the sample itself.

All the following plots were created with MS Excel ®.

7.1 Diesel/Biodiesel results

This section deals with the measurement results from mixtures of Diesel and Biodiesel only.

7.1.1 Square sample container results

These measurements were carried out by the use of square sample containers. Figure 33 shows the measured signal of 3 experiments, with 3 test runs of the 1st and 2nd experiment, and 2 test runs of the 3rd. The samples were mixed in 10% steps (increase of Biodiesel fraction of 10% at each step).

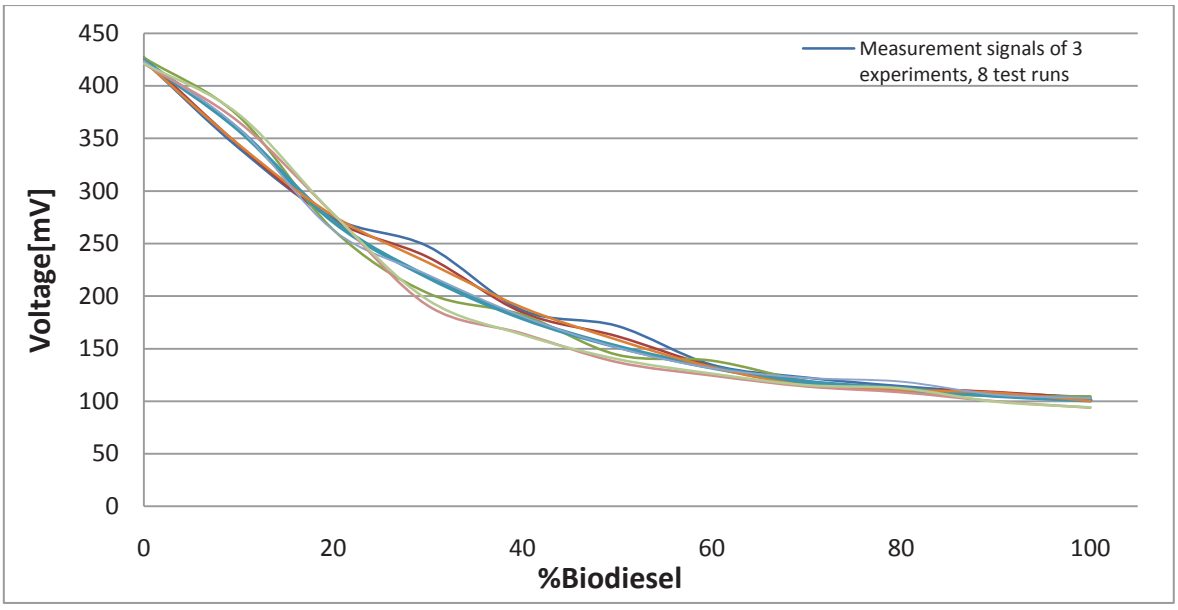

Figure 33: Measurement signals from Diesel/Biodiesel mixtures (square containers)

As one can see, the results are more or less accurately reproducible. The main deviations in the measured signal were located at Biodiesel percentages between 30% and 50%. The reasons for the deviations cannot be clearly described. Probably these errors arise from

inaccurate sample preparation. The reason for that is that the square sample containers are of very small volume, which makes highly accurate mixing difficult.

There is also a non linear behavior observed. It is clear that the absorption behavior in this range (30% and 50% Biodiesel) differs from the overall behavior. This fact may be due to newly formed compounds with different absorption behavior, which start forming at the 30% Biodiesel fraction, and become saturated with no further compound forming at the 50% Biodiesel fraction.

Figure 34 shows the interval error and value error of Diesel/Biodiesel mixtures.

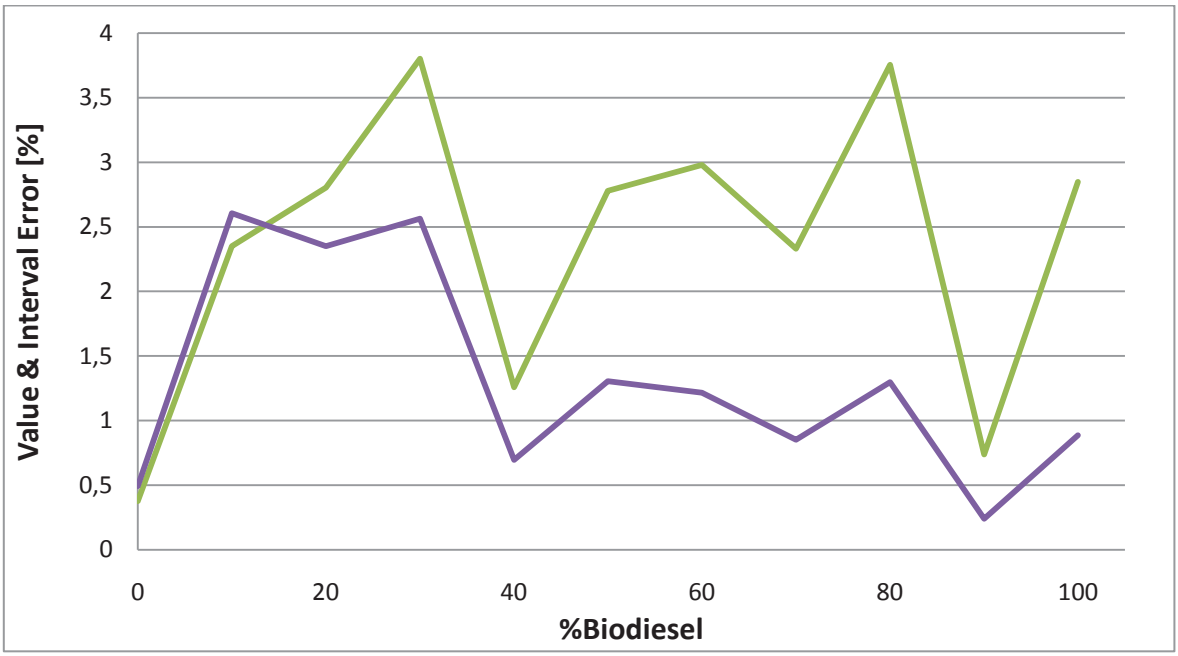

Figure 34: Diesel/Biodiesel: Interval error (purple line) and Value error (green line) for square containers

As one can see, the maximum value error is slightly above 3.5%, and the interval error at 2.5%. The interval here is 323.41 mV. The results for the Diesel/Biodiesel mixtures are very nice, since the highest error is 3.5%, which means that the mixing ratio can be determined accurately, without correction factors.

7.1.2 Round sample container results

The measurements with round sample containers show the same behavior as with the square containers. The main difference is the fact that the signal of the latter is higher, because of focusing of the incident light, and the calculated errors are lower. Figure 35 shows the measurement results of 2 experiments with 2 test runs respectively. Here, the experiments were mixed in 5% additional Biodiesel fraction steps.

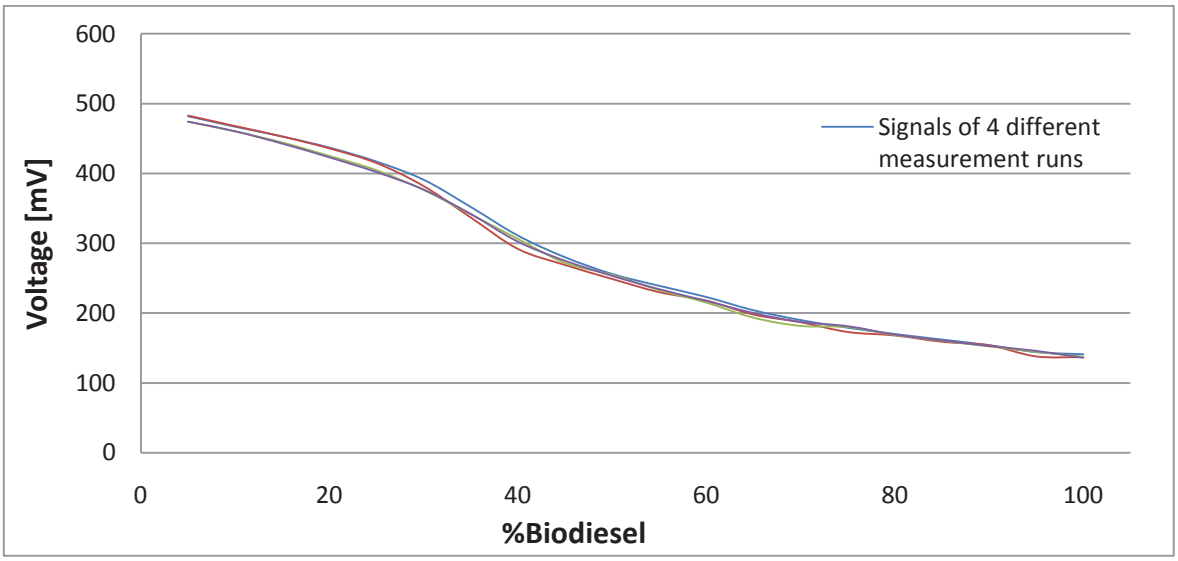

Figure 35: Measurement signals from Diesel/Biodiesel mixtures (round containers)

Again, one can see the nonlinear behavior in the 35% to 50% Biodiesel region, with the same reason as stated before. In addition to that, it is obvious, that the signal is more stable than with the square sample containers.

Figure 36 shows the value error and the interval error of the measurement runs.

Figure 36: Diesel/Biodiesel: Interval error (purple line) and Value error (green line) for round containers

One can see that the value error is at a maximum of slightly above 2.5% and slightly below 2.5% respectively for the interval error. This result is accurate enough for fulfilling the task of a fuel detector.

7.2 Diesel/Cracked Gas Oil results

This chapter deals with the measurement results of Diesel/Cracked Gas Oil mixtures. The procedure was the same as with Biodiesel. Moreover, both available sample containers were used.

7.2.1 Square sample container results

The measurements for the Diesel/Cracked Gas oil mixtures consist of 2 experiments with 3 test runs each. The samples were prepared with 10% additional CGO fraction steps. Figure 37 shows the measured voltage vs. Cracked Gas Oil percentage.

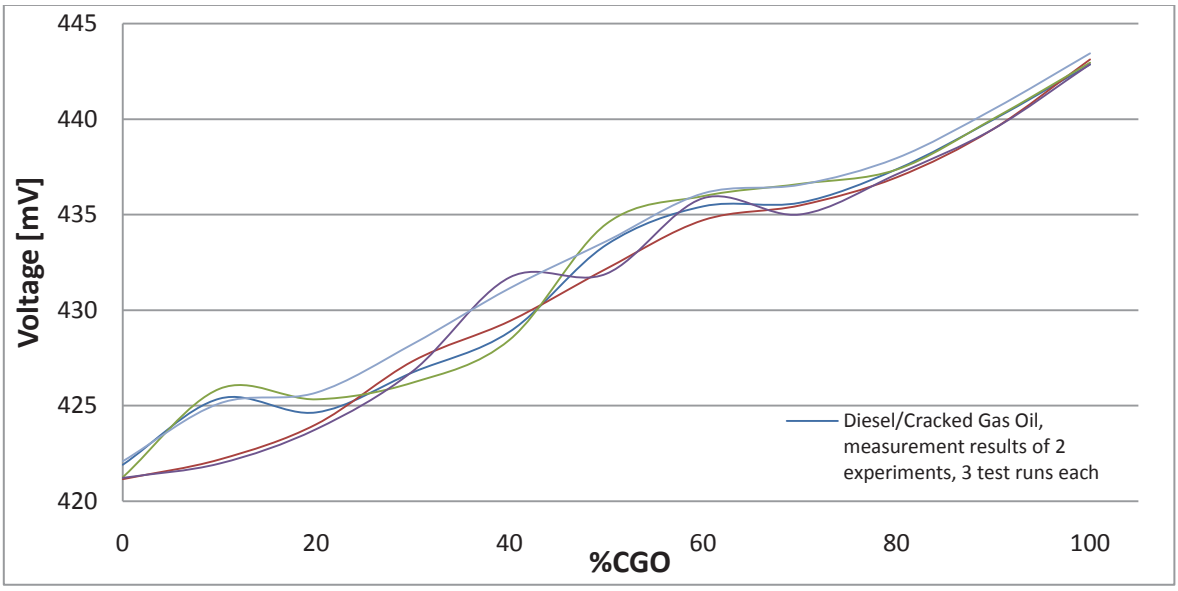

Figure 37: Measurement signals from Diesel/Cracked Gas Oil mixtures (square containers)

One can see in the figure above that the measured voltage is fluctuating, but a general trend can be recognized. The reasons for the fluctuations are unclear, because too many factors (see section 7) influence the results. Nevertheless it is probable that the manual mixing error has a high influence.

Also important is the small measured interval, which is just 21.36 mV in this case. This is the reason for the relatively high interval error. The value error and the interval error can be seen in figure 38.

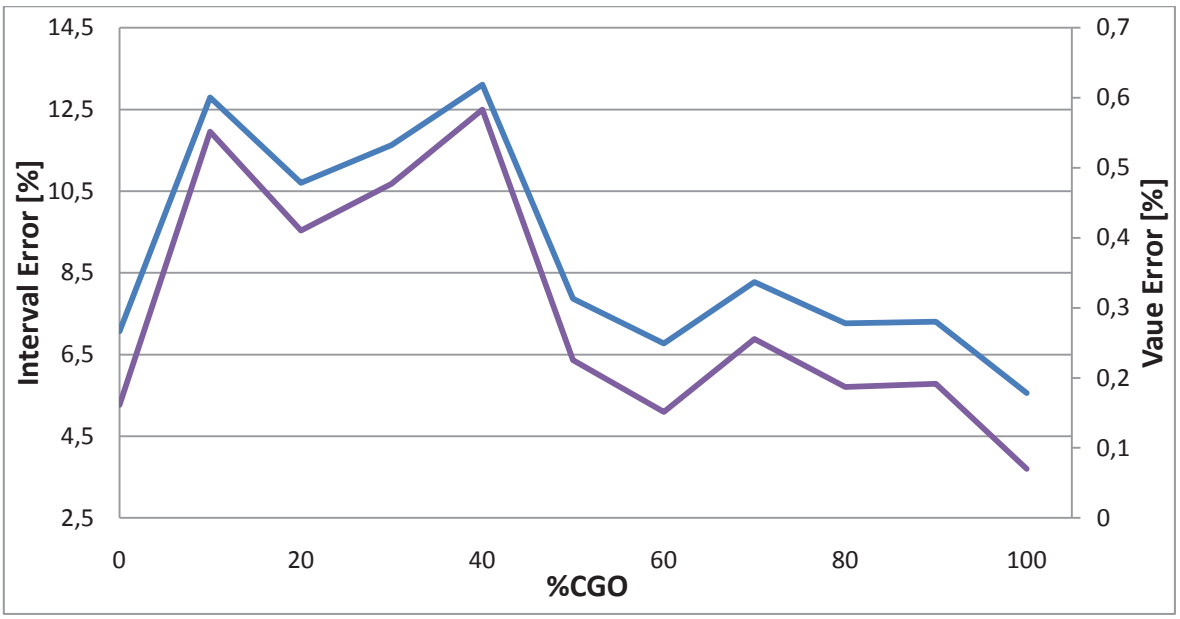

Figure 38: Diesel/Cracked Gas Oil: Interval error (purple line) and Value error (blue line) for square containers

In the figure above, one can see that the value error is low, but not insignificant. The interval error is relatively high, because the interval of the measurements is small (rule of thumb: the smaller the interval, the higher the resulting error of very small changes). It must be stated here, that the Cracked Gas Oil results for square sample containers have a high improvement potential, since the measurements with the round sample containers give much better results.

7.2.2 Round sample container results

The measurements for the Diesel/Cracked Gas oil mixtures by use of round sample containers consist of 3 experiments with 3 test runs each. The samples were prepared with 10% additional CGO fraction steps. Figure 39 shows the measured voltage vs. Cracked Gas Oil percentage.

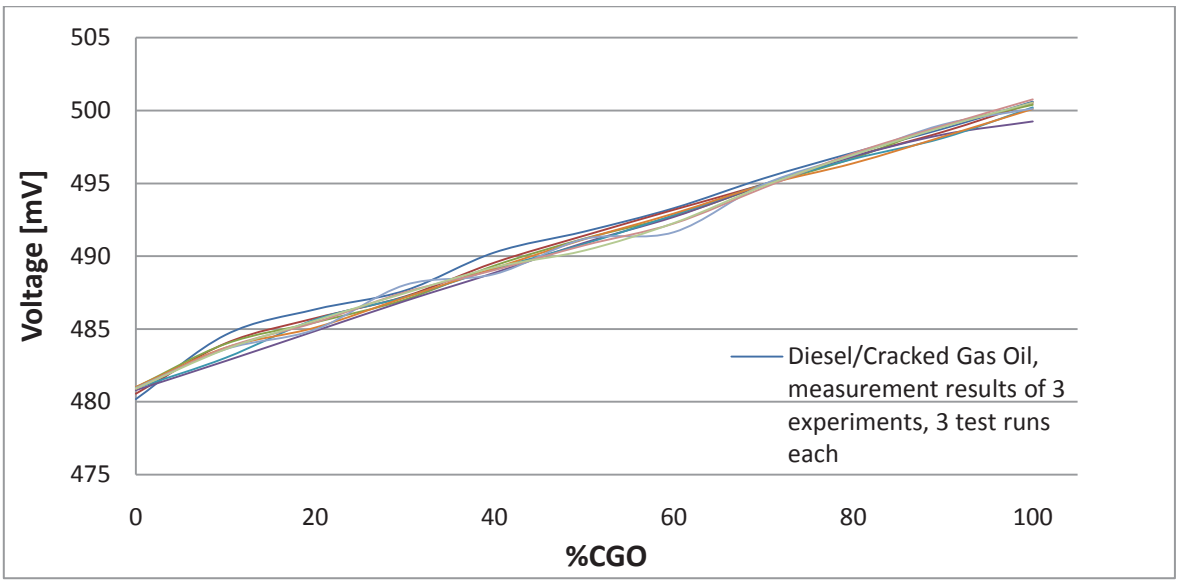

Figure 39: Measurement signals from Diesel/Cracked Gas Oil mixtures (round containers)

These results show a very strong linear relationship. As one can see, the test runs only differ marginally from each other. This is a fact which makes the fuel detector suitable for distinguishing the mixing ratios of Diesel and Cracked Gas Oil.

Figure 40 shows the interval error and the value error.

One can see in the figure below that the highest average error (the interval error in this case) is lower than 1.8%. This indicates a stable function of the device itself and accurate measurements.

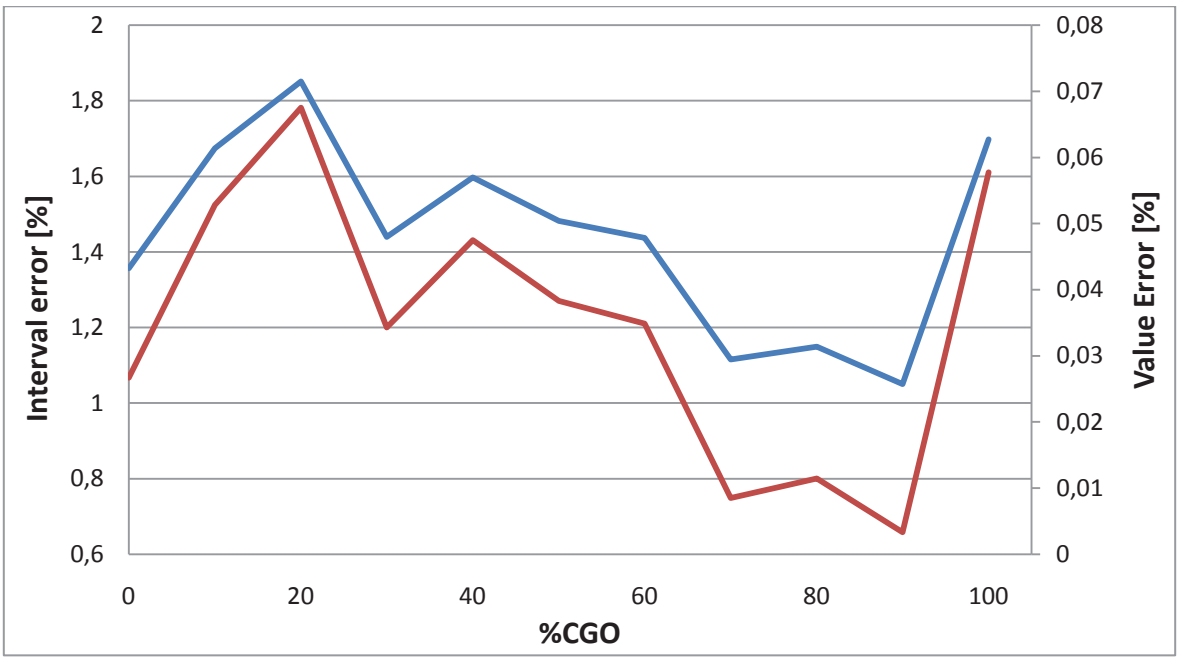

Figure 40: Diesel/Cracked Gas Oil: Interval error (red line) and Value error (blue line) for round containers

7.3 Diesel/Kerosene results

This section deals with the measurement results of Diesel/Kerosene mixtures only. The measurements were carried out with 10% additional Kerosene fraction steps.

7.3.1 Square sample container results

The measurements for the Diesel/Kerosene mixtures by use of square sample containers consist of 3 experiments with overall 5 test runs. The samples were prepared with 10% additional Kerosene fraction steps. Figure 41 shows the measured voltage vs. Kerosene percentage.

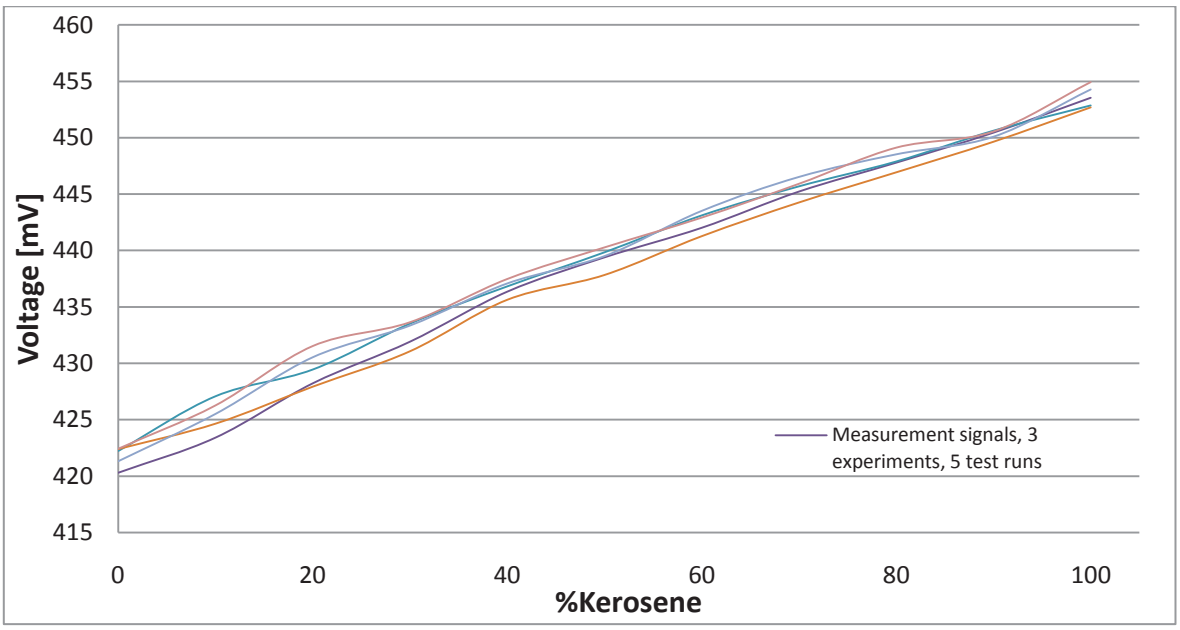

Figure 41: Measurement signals from Diesel/Kerosene mixtures (square containers)

The figure above shows a linear relationship between the Kerosene percentage and the measured voltage. The deviations in the voltage outputs can be caused by preparation errors, or ambient light. Anyway, the results show a good reproducibility within the small average measured voltage interval, which is in this case 29.67 mV. Additional corrections seem to have a good chance of increasing the accuracy of the measurements even further.

Figure 42 shows the value error and the interval error of the Diesel/Kerosene measurements.

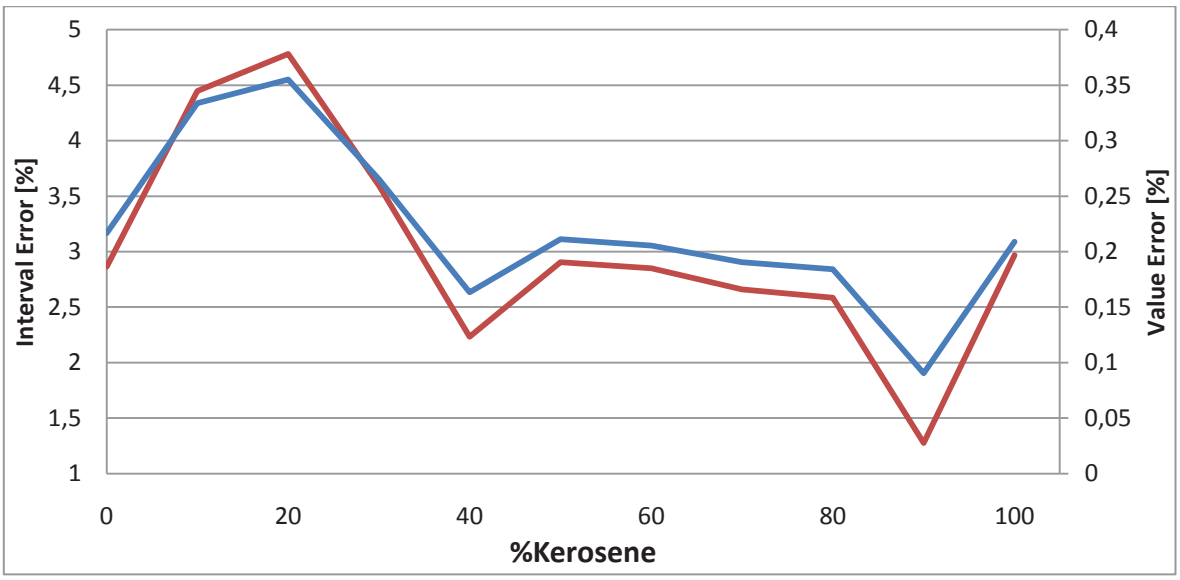

Figure 42: Diesel/Kerosene: Interval error (red line) and Value error (blue line) for square containers

This plot shows the interval error, which has its maximum at roughly 4.8%, and the value error with a maximum value of 0.35%. Again, the errors are believed to be reducible by additional correction factors.

7.3.2 Round sample container results

The test utilizing round sample containers was carried out for fuel mixtures with 10% additional Kerosene fraction steps. The measurements have been done for 3 experiments with 4 test runs each. Again, the round sample containers provided better results than the square containers. Figure 43 shows the results of these measurements.

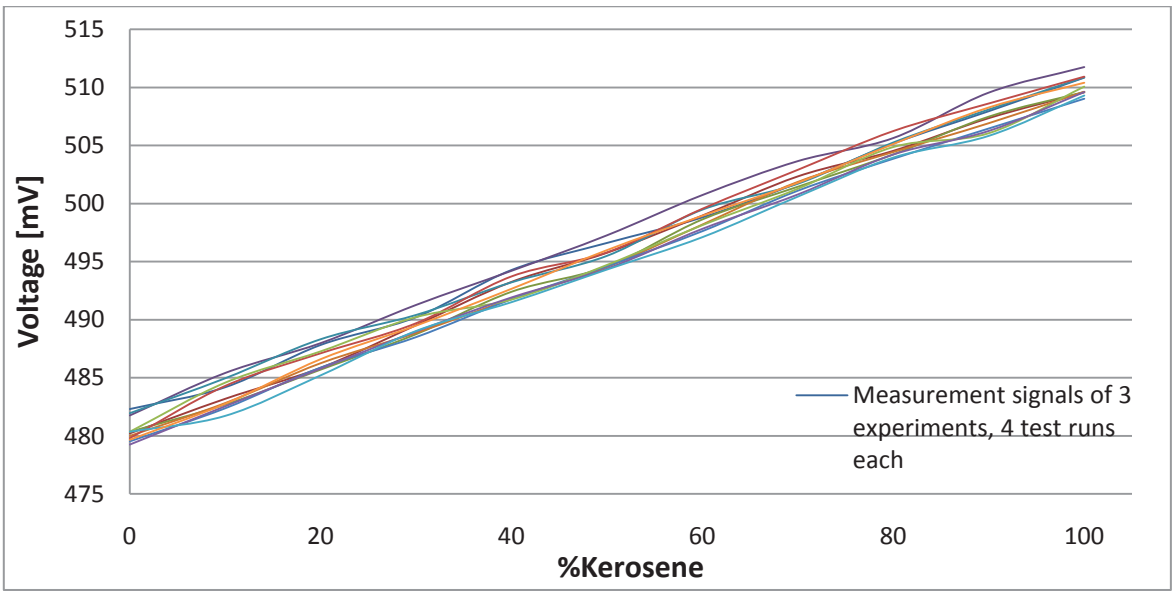

Figure 43: Measurement signals from Diesel/Kerosene mixtures (round containers)

These measurements have shown a very strong linear relationship, with relatively small deviations in the voltage output. A good reproducibility is also given, since 12 test runs were carried out which gave more or less the same results. Figure 44 shows the value error and the interval error.

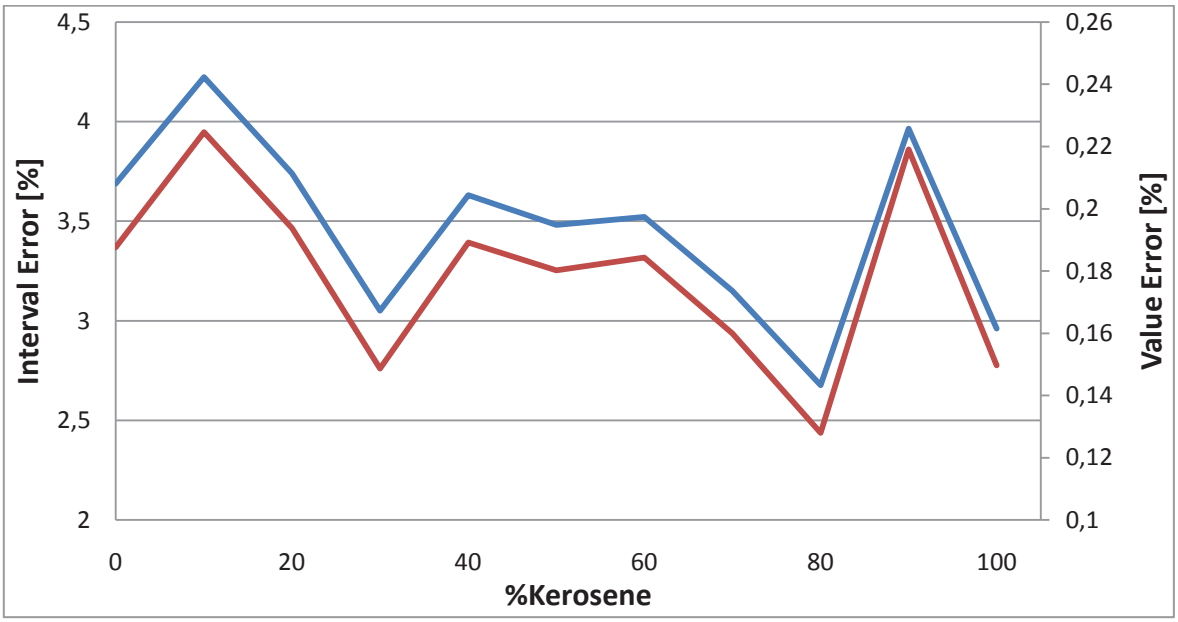

Figure 44: Diesel/Kerosene: Interval error (red line) and Value error (blue line) for round containers

The figure above reveals that the maximum error is about 4%, which means that the round sample containers perform about 1% better than the square containers. Since the average measured voltage interval is 29.67 mV, the 4% interval error is a good result, because no correction factors were implemented.

7.4 Diesel/Gasoline results

This section deals with the measurement results of Diesel/Gasoline mixtures only. The measurements were carried out with 10% additional Gasoline fraction steps. Because of the aggressive reaction of the Gasoline with the square sample containers, which were made of plastic, the measurements were carried out with the round sample containers, made of glass, only. The results can also be inaccurate, because of the easy evaporation of the gasoline. This means, that probably an unspecified fraction of the Gasoline evaporated during the measurements.

7.4.1 Round sample container results

The test utilizing round sample containers was carried out for fuel mixtures with 10% additional Gasoline fraction steps. The measurements have been done for 3 experiments with 3 test runs each. Figure 45 shows the measured voltages vs. Gasoline percentage.

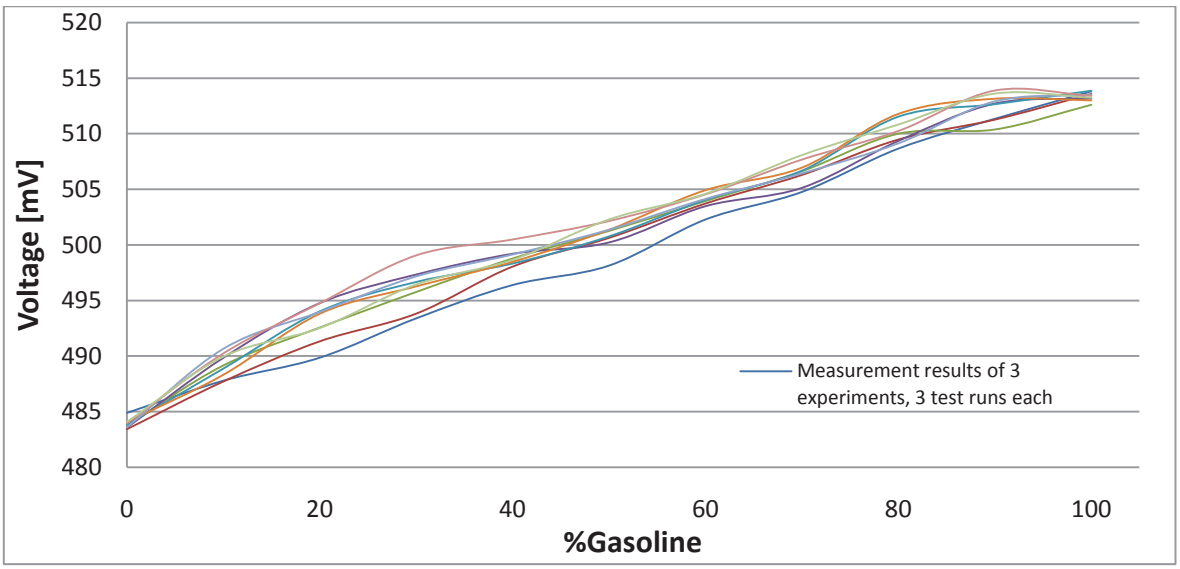

Figure 45: Measurement signals from Diesel/Gasoline mixtures (round containers)

The most severe deviations appear in the 20% - 50% Gasoline region, which may be related to the gasoline evaporation. Besides that, the measurements show a linear behavior. Since the average measured voltage interval is 29.44 mV, the detectors respond to the increasing Gasoline fraction is satisfying. Figure 46 shows the interval error and the value error vs. Gasoline percentage.

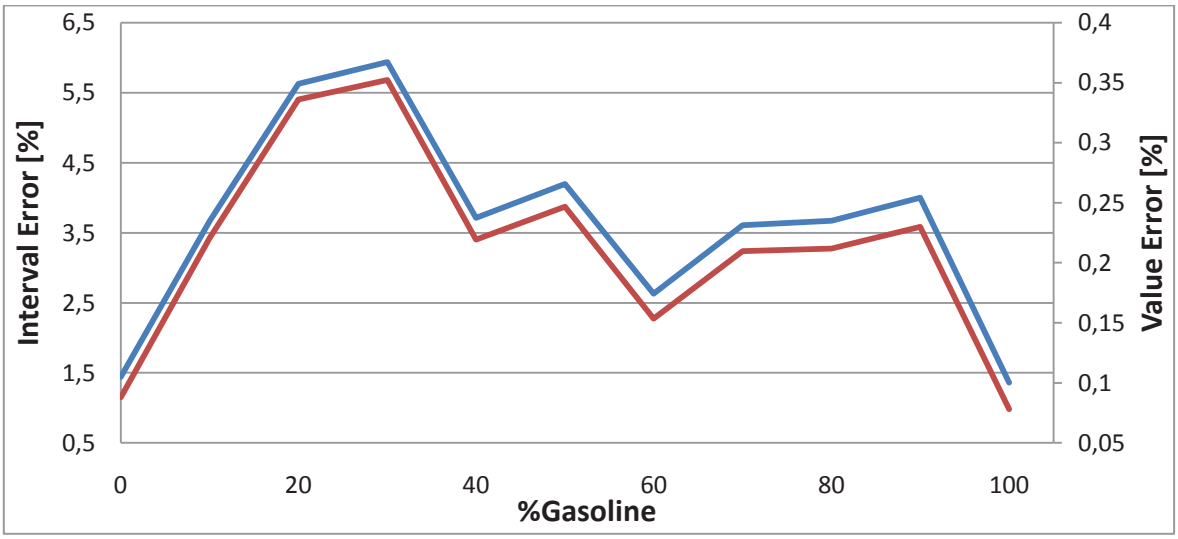

Figure 46: Diesel/Gasoline: Interval error (blue line) and Value error (red line) for round containers

As one can see, the interval error is about 6% at its maximum. Once again it is stated, that no correction factors are included, which would highly increase the accuracy of the measurements. Prohibiting the evaporation of the Gasoline would eliminate this error source, which was not quantified for the test run durations.

7.5 Diesel/Fuel Oil results

For the sake of completeness, measurement runs were carried out for Diesel/Fuel Oil mixtures. Generally Fuel Oil is colored Diesel, so no big differences in the voltage output between 100% Diesel and 0% Diesel were expected. This was then confirmed by the measurement results. In addition to that, the measurements were carried out with round sample containers only.

7.5.1 Round sample container results

Here the samples were prepared in 25% additional Fuel Oil fraction steps, because of the low expected differences in the voltage outputs. Figure 47 shows the measured voltage output vs. Fuel Oil percentage.

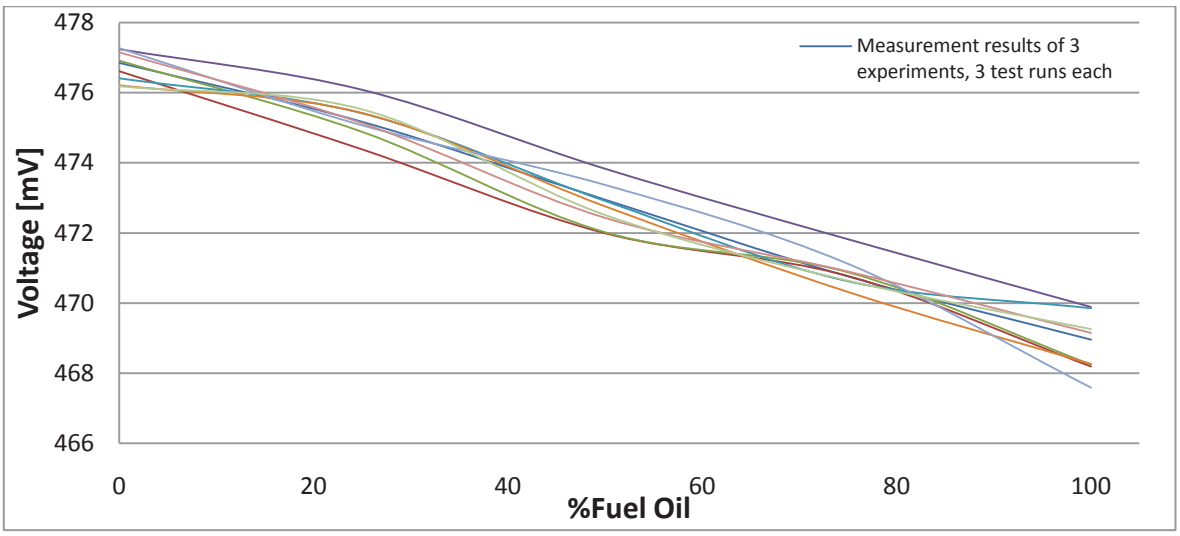

Figure 47: Measurement signals from Diesel/Fuel Oil mixtures (round containers)

As one can see, the results show a linear relationship between the measured voltage and the Fuel Oil fraction. The problem with the Diesel/Fuel Oil measurements is the very small voltage interval, with is here just 7.93 mV. This means that an output error of just 0.8 mV already results in an error of 10%. This makes this result very interesting, as a difference in every test run was detected even at this small interval, which shows that the applied detection method is able to detect even smallest changes in composition, even for very similar test fuels. Figure 48 shows the interval error and the value error of the measurements.

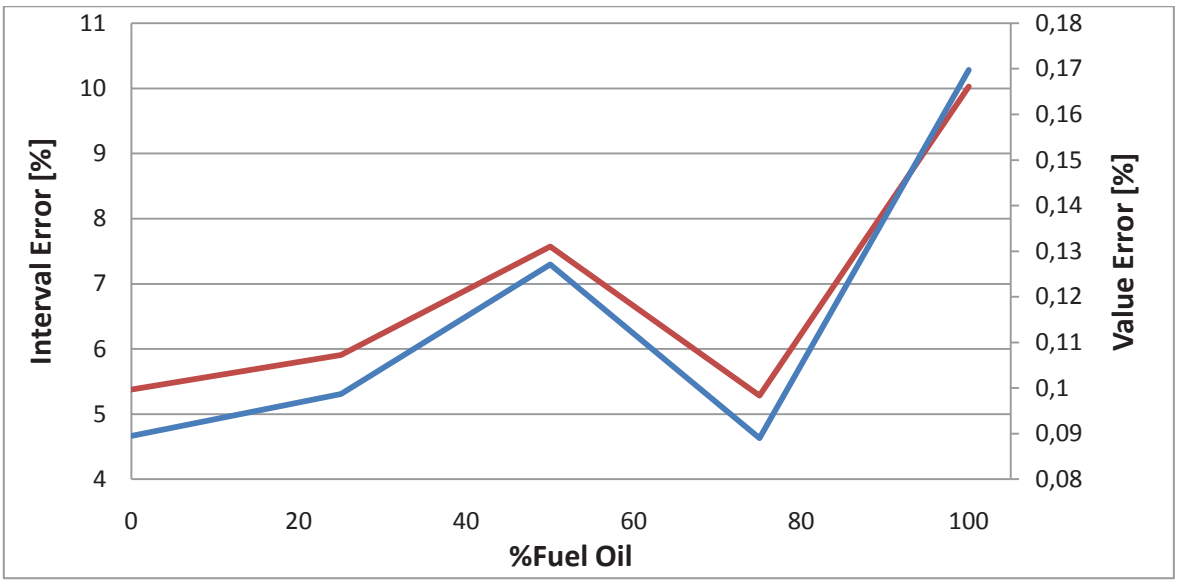

Figure 48: Diesel/Fuel Oil: Interval error (red line) and Value error (blue line) for round containers

The interval error is between 6% and 10%, which is a good result, due to the fact, as stated before, that the interval is that small.

8 Conclusion

Based on the presented results, the task of finding a proper fuel detector is believed to be accomplished. It is suggested to do a further evaluation of the method by searching for correction factors for the different error sources. Especially a temperature correction would increase the accuracy of the measurements. In addition to that, it seems that the device is able to deliver calibration curves for even more, different fuel mixtures. So test runs with, for example Kerosene/Cracked Gas Oil mixtures, would also give usable results.

Since only binary mixtures were evaluated, tests of mixtures with 3 components can also be worth the effort.

Based on the test runs with different sample container shapes, it is recommended to develop a cylindrically shaped device, since the round sample containers always gave the better results. In addition to that, a round device is believed to be more applicable in an automobile, since it can be inserted along the fuel line, with low space consumption.

More detail on the results of the tested fuel mixtures is given here:

- The measurements of Diesel/Biodiesel mixtures give very accurate results. Because of the high measured voltage interval, inaccuracies in the measurement do not severely influence the results representing the Biodiesel fraction of the mixture. Round sample containers give better results. The interval error is lower than 2.5%.

- The Diesel/Cracked Gas Oil mixtures are highly fluctuating in the results with square sample containers, which make the determination of the Cracked Gas Oil fraction of the mixture difficult. On the other hand, measurements using the round sample containers are highly accurate with an interval error of just 1.8% at its maximum. This means that the measurement method can be used for the given task, even without several (but still recommended) correction factors.

- Diesel/Kerosene mixtures were tested with both sample container shapes. Again it turned out, that the round containers perform better than the square ones. As stated before, an interval error of 4.8% was achieved. Here, the application of a

correction factor for temperature is believed to highly reduce the error. Nevertheless, the results show a good linear relation between the measured voltage and the Kerosene fraction of the mixture, which makes the absorption method applicable for the given task.

- Test results of Diesel/Gasoline mixtures show a linear relationship as well. The measurements were carried out using round sample containers only, so no comparison of the different container shapes can be given. As the evaporation of the Gasoline fraction was identified to be an error source, retesting of Diesel/Gasoline mixtures under conditions which prohibit evaporation are recommended. Nevertheless, the absorption method has shown its ability to detect Diesel/Gasoline fractions with a maximum interval error of 6%.

- Diesel/Fuel Oil mixtures were tested for the sake of completeness. It turned out that the measurement of very similar test fuels is also possible. The interval error is relatively high because of the small measured voltage interval of just 7.9mV, but the value error is very small (see figure 48). Additional test runs for the Diesel/Fuel Oil mixtures are recommended. It is probable that the applied absorption method will also be accurate enough to detect the mixture fractions of Diesel and Fuel Oil.

The named reasons enable the application of the absorption method for a device used in an automobile.

References

[1]http://www.physik.unibas.ch/Praktikum/VPII/Fluoreszenz/Fluorescence_and_Phosphorescence.pdf, accessed on the 15.10.2008

[2] http://dictionary.reference.com/search?q=orbital&db=luna, accessed on the 27.04.2009

[3] A.T Rhys-Williams, "An introduction to fluorescence spectroscopy", PerkinElmer Ltd. , 2000

[4] http://instructor.physics.lsa.umich.edu/adv-labs/Raman_Spectroscopy/Raman_spect.pdf, accessed on the 25.10.2008

[5] http://en.wikipedia.org/wiki/File:Raman_energy_levels.jpg, accessed on the 22.10.2008

[6] Digambra Patra, A.K. Mishra, "Study of Diesel fuel contamination by excitation emission matrix spectral subtraction fluorescence", Analytica Chimina Acta 454 (2002), p 209-215

[7] Wayne Smith, Stuart Farquharson, "A portable fuel analyser", Advanced Environmental, Chemical and Biological Sensing Technologies IV (2006)

[8] Digambra Patra, A.K. Mishra, "Total synchronous fluorescence scan spectra of petroleum products" Springer Verlag 2002

[9] Axel Munack, Jürgen Krahl, "Erkennung des RME-Betriebes mittels eines Biodiesel Kraftstoffsensors", FAL Agricultural research, Special Issue 257, 2003

[10] Datasheet of the L-7104 PBC-Z LED by Kingbright (found at the delivered CD)

[11] Datasheet of the EPD-520-5/0.5 photodiode by Epigap (found at the delivered CD)

[12] B. Falter "Elektronik und analoge Schaltungstechnik", script at the BTU Cottbus, Faculty 3

[13] Kolle, Christian "Development and evaluation of a phase fluorometric Instrumentation for luminescence based optical oxygen sensors", Doctor´s Thesis, University of Leoben, 1999

[14] http://de.wikipedia.org/wiki/Operationsverstärker accessed on the 20.12.2008

[15] http://en.wikipedia.org/wiki/Snell's_law accessed on the 15.01.2009

Appendices

[Geben Sie hier den Text ein].